

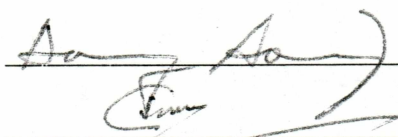
ANALYTICAL AND NUMERICAL STUDIES ON MACRO AND MICRO SCALE

HEAT SINKS FOR ELECTRONIC APPLICATIONS

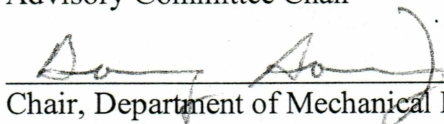
By

Devdatta P. Kulkarni

RECOMMENDED:




Debendra K. Das
Advisory Committee Chair

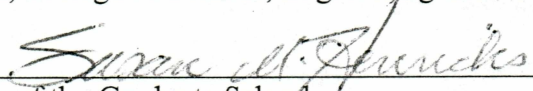


Chair, Department of Mechanical Engineering

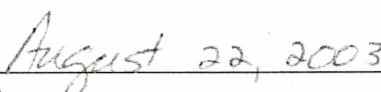
APPROVED:



Dean, College of Science, Engineering and Mathematics



Dean of the Graduate School



Date

ANALYTICAL AND NUMERICAL STUDIES ON MACRO AND MICRO SCALE
HEAT SINKS FOR ELECTRONICS APPLICATIONS

A
THESIS

Presented to the Faculty
of the University of Alaska Fairbanks

In Partial Fulfillment of the Requirements
for the Degree of

MASTER OF SCIENCE

By

Devdatta P. Kulkarni, B.E.

Fairbanks, Alaska

August 2003

Tk
7870.25
K85
2003

ABSTRACT

From the practice in computer industry the standard approach for electronics cooling is fan-cooled heat sinks. We developed thermal models for forced convection heat sinks. An Intel Pentium III chip has been adopted as a preliminary design case to develop necessary equations. We found the heat dissipated from the aluminum heat sink, based upon different modes of airflow over the fins. We also considered radiation heat transfer. We performed transient heat transfer analysis to determine the time to attain the steady state temperature for the whole system for macro and microscale also. Next, we refined our one-dimensional analytical convection analysis using the numerical analysis. This was done using the computational fluid dynamics code Fluent to obtain accurate velocity fields over the fins. Using these improved velocities, convective heat transfer coefficients were computed. Next, we have miniaturized the processor chip size to the micrometer scale and have designed a heat sink based upon the models we have developed. Calculations of mean free path and Knudsen number shows the continuum theory for air still holds for our designed micro-channels. Equations for natural convection heat sinks are also explored as a part of this study. In the microscale study, we did forced and natural convection analysis.

Table of Contents

| Chapter | Title | Page |
|---------|--|------|
| | Signature Page | i |
| | Title Page | ii |
| | Abstract | iii |
| | Table of Contents | iv |
| | List of Figures | viii |
| | List of Tables | x |
| | Nomenclature | xi |
| | Acknowledgements | xiii |
| | Dedication | xiv |
| 1 | INTRODUCTION | 1 |
| 2 | THEORY | 5 |
| | 2.1 Heat Conduction in Chips and Substrates | 5 |
| | 2.2 Temperature Distribution in a Processor Chip Generating Heat | 5 |
| | 2.3 Transient Heat Conduction in the Chip and the Heat Sink | 6 |
| | 2.4 Interface/Contact Resistance | 7 |
| | 2.5 Spreading Resistance | 8 |
| | 2.6 Heat Transfer via Convection from the Heat Sink | 8 |
| | 2.6.1 Forced Convection Analysis | 9 |
| | 2.6.2 Natural Convection Analysis | 9 |
| | 2.7 Heat Transfer from the Fins of a Heat Sink | 10 |
| | 2.8 Radiation Heat Transfer from Heat Sinks | 11 |

| | | |
|-------|--|----|
| 3 | ANALYTICAL SOLUTIONS FOR MACRO SCALE CHIP | 13 |
| 3.1 | Model Description | 14 |
| 3.2 | Conduction Analysis | 16 |
| 3.2.1 | Heat Conduction to the Printed Circuit Board | 16 |
| 3.2.2 | Temperature Distribution in the Chip from Heat Generation Theory | 17 |
| 3.2.3 | Interface Resistance with a Bond Material | 19 |
| 3.2.4 | Spreading Resistance to the Substrate | 21 |
| 3.2.5 | Steady State Heat Conduction in the Heat Sink Base | 22 |
| 3.2.6 | Transient Heat Conduction in the System | 23 |
| 3.3 | Convection Analysis | 25 |
| 3.3.1 | Calculation of Air Velocity | 25 |
| 3.3.2 | Reynolds Number | 26 |
| 3.3.3 | Nusselt Number | 26 |
| 3.3.4 | Heat Transfer Coefficient | 27 |
| 3.4 | Heat Loss from Fins | 27 |
| 3.4.1 | Convection Results | 29 |
| 3.5 | Radiation Analysis | 30 |
| 3.5.1 | Effect of Different Emissivity | 33 |
| 3.6 | Natural Convection Case: Pentium II Analysis | 35 |
| 3.6.1 | Radiation Analysis in Pentium II Fins | 39 |
| 3.7 | Boundary Layer Thickness | 40 |
| 3.7.1 | Refinement of Heat Loss from Fins | 43 |
| 3.8 | Numerical Analysis | 43 |
| 3.8.1 | Introduction | 43 |
| 3.8.2 | Problem Description in a Two Dimensional Domain | 45 |
| 3.8.3 | Computational Domain | 46 |
| 3.8.4 | Mesh Generation | 46 |
| 3.8.5 | Post Processing of Results | 49 |

| | | |
|-------|--|----|
| 3.8.6 | Three Dimensional Analysis | 53 |
| 3.8.7 | Post Processing of 3D Results | 55 |
| 4 | APPLICATION TO MICROSCALE CHIPS | 57 |
| 4.1 | Specifications | 57 |
| 4.1.1 | Scaled Dimensions | 57 |
| 4.2 | Need for the Heat Sink | 58 |
| 4.3 | Conduction Analysis for the Miniaturized Chip and Sink | 59 |
| 4.3.1 | Temperature Distribution in the Chip from Heat Generation Theory | 59 |
| 4.3.2 | Interface Resistance with a Bond Material | 60 |
| 4.3.3 | Spreading Resistance to the Substrate | 60 |
| 4.3.4 | Steady State Heat Conduction in the Sink Base | 62 |
| 4.4 | Transient Heat Conduction | 63 |
| 4.5 | Steady State Gas Flow Model | 64 |
| 4.5.1 | Mean Free Path Calculation for the Air Molecules | 65 |
| 4.5.2 | Verification of the Existing Model | 68 |
| 4.6 | Convection Analysis Related to Microchip | 69 |
| 4.6.1 | Calculation of Air Velocity | 69 |
| 4.6.2 | Reynolds Number | 70 |
| 4.6.3 | Nusselts Number | 70 |
| 4.6.4 | Heat Transfer Coefficient | 70 |
| 4.7 | Heat Loss From Fins of Micro Heat Sink | 71 |
| 4.8 | Convection Results | 71 |
| 4.9 | Radiation Analysis in Microchannels | 72 |
| 4.9.1 | Effect of Varying Emissivity | 74 |
| 4.10 | Alternate Design of the Heat Sink for Microchip | 75 |

| | | |
|---|--|----|
| | 4.11 Numerical Analysis for Micro Scale Modeling | 77 |
| | 4.11.1 Reynolds Number Matching | 77 |
| 5 | CONCLUSIONS | 80 |
| | REFERENCES | 82 |

LIST OF FIGURES

| | |
|--|----|
| Figure 2.1 Schematic to Represent Contact Resistance | 7 |
| Figure 2.2 Schematic of the Chip Placement on a Substrate | 8 |
| Figure 2.3 Schematic of Dimensions of the Fins facing each other for View Factor Determination | 12 |
| Figure 3.1(a) Layout of Pentium III Chip with Heat Sink and Fan Assembly | 15 |
| Figure 3.1(b) Important Dimensions of the Heat Sink Geometry | 16 |
| Figure 3.2 Schematic of Die Placement over the Substrate with <u>Underfill</u> | 17 |
| Figure 3.3 Schematic Diagram of Chip Placement | 18 |
| Figure 3.4 Temperature Profile in the Processor Chip | 19 |
| Figure 3.5 Two-Dimensional Schematic View of Spreading Resistance | 21 |
| Figure 3.6 The Heat Flow Network with Different Resistances | 24 |
| Figure 3.7 Temperature Rise in Chip and Heat Sink System until Steady State is Achieved | 25 |
| Figure 3.8 Schematic of Airflow over the Fns | 26 |
| Figure 3.9 Schematic of Channel Surfaces for Radiation | 30 |
| Figure 3.10 Schematic to find View Factor for Two Rectangular Surfaces Sharing a Common Side | 31 |
| Figure 3.11 Distribution of Radiation Loss | 32 |
| Figure 3.12 Effect of Different Emissivities | 34 |
| Figure 3.13 Layout of Pentium II Processor with Heat Sink | 35 |
| Figure 3.14(a) Schematic of Fins with Different Dimensions | 36 |
| Figure 3.14(b) Side Schematic of Fins for Pentium II Processor | 37 |
| Figure 3.15 Effect of Surface Temperature on Heat Loss from Fins | 39 |
| Figure 3.16 Schematic of Boundary Layer Development | 40 |
| Figure 3.17 Development of Boundary Layer for Different Velocities | 41 |
| Figure 3.18 Variation of Heat Transfer Coefficient h from Leading Edge | 42 |

| | |
|---|----|
| Figure 3.19 Details of Grid Generation | 47 |
| Figure 3.20 Velocity Distribution over a Fin with Inlet Velocity of 3.3585 m/s | 49 |
| Figure 3.21 Velocity Distribution at Various Cross Sections of y with Inlet Velocity of 2.14 m/s | 50 |
| Figure 3.22 Velocity Distribution at Various Cross Sections of y with Inlet Velocity of 3.3585 m/s | 51 |
| Figure 3.23 Computational Domain for 3D Analysis | 53 |
| Figure 3.24 Contours of Heat Transfer Coefficient over the Fin Surface for a Velocity of 3.35 m/s | 55 |
| Figure 3.25 Contours of Heat Transfer Coefficient over the Fin Surface for a Velocity of 2.14 m/s | 56 |
| Figure 4.1 Scaled Heat Sink Geometry with Dimensions in Micrometers | 58 |
| Figure 4.2 Change in Temperature (milli Kelvin) Profile in the Processor Chip | 60 |
| Figure 4.3 Schematic of Heat Spreading Cone | 61 |
| Figure 4.4 Temperature Rise in the Total Heat Sink until Steady State is Achieved | 63 |
| Figure 4.5 Variation of Heat Loss with Varying Airflow over the Heat Sink | 72 |
| Figure 4.6 Distribution of Radiation Loss in Micro Heat sink | 74 |
| Figure 4.7 Effect on Heat Loss by Radiation with Different Emissivities | 75 |
| Figure 4.8 Effect of Varying Fin Surface Temperature on Heat Loss by Free Convection and Radiation | 76 |
| Figure 4.9 Counters of Velocity for Microscale Fins | 78 |
| Figure 4.10 Contours of Surface Heat Transfer over the Fin for Velocity of 1.4 cm/s | 79 |

LIST OF TABLES

| | |
|--|----|
| Table 3.1 Thermal Properties of Interface Materials | 20 |
| Table 3.2 Comparisons of Convection Heat Losses for Various Cases | 29 |
| Table 3.3 View Factor for Various Faces | 32 |
| Table 3.4 Materials with High Emissivity Used in Electronic industry | 33 |
| Table 3.5 Heat Loss from One Fin for 2.14 m/s Velocity at 45 Deg C | 52 |
| Table 3.6 Heat Loss from One Fin for 3.3585 m/s Velocity at 45 Deg C | 52 |
| Table 4.1 Criteria for Different Fluid Regime | 65 |
| Table 4.2 Knudsen Numbers for Different Models | 69 |
| Table 4.3 Comparison of Convection Heat Losses for Various Cases | 71 |

NOMENCLATURE

| | |
|------------|--|
| A_x | Cross sectional area, m^2 |
| c_p | Specific Heat, $J/kg\ ^\circ C$ |
| D | Distance between two objects, m |
| F_{1-2} | View Factor |
| h | Heat Transfer Coefficient, $W/m^2\ ^\circ C$ |
| k | Thermal conductivity of material, W/mK |
| k_a | Thermal conductivity of air, W/mK |
| L | Length of object, m |
| L_1 | Characteristics length, m |
| M | Mass of component, Kg |
| P | Perimeter, m |
| p | Pressure, Pascal |
| Pr | Prandtl number |
| q | Heat Transfer Rate, W |
| q_G | Heat generated, W |
| q'' | Heat Flux, W/m^2 |
| q''' | Rate of internal energy generation, W/m^3 |
| R_c'' | Contact resistance per unit area, $m^2\ K/W$ |
| R_c'' | Interface resistance, $m^2\ K/W$ |
| Re_L | Reynolds number |
| T | Temperature of surface, $^\circ C/^\circ K$ |
| T_o | Initial temperature, $^\circ C$ |
| T_f | Fin tip temperature, $^\circ C$ |
| T_s | Surface Temperature, $^\circ C$ |
| T_∞ | Fluid Temperature, $^\circ C$ |
| U | Velocity of air, m/s |

| | |
|-----|----------------------------|
| u | Inlet Velocity of air, m/s |
| v | Velocity of fluid, m/s |
| x | Distance in x direction, m |

GREEK LETTERS

| | |
|---------------|--|
| ε | Emissivity of material |
| ρ | Density of fluid, kg /m ³ |
| μ | Dynamic Viscosity of fluid, N s/m ² |
| ν | Kinematic viscosity of fluid, m ² /s = μ / ρ |
| σ | Stefan-Boltzman constant, W/m ² K ⁴ |

Acknowledgements

It gives me a great pleasure to thank those many people who made this thesis possible. I am indebted to Dr. Debendra K. Das who as a faculty advisor supervised this research, provided great ideas, suggestions and encouragements when problem arose, and devoted his valuable time for the discussions and comments during the writing phase of this thesis. My appreciation goes to my other committee members Dr. Douglas Goering and Dr. Gautam Sarakar for helping me further and giving me some new ideas and sharing their time. Thanks to all of you for your guidance and assistance.

This work is supported by the Center for Nanosensor Technology, University of Alaska Fairbanks, under the contract DMEA90-02-C-0226.

I would also like to express my gratitude to Mr. Srivathsan Ragunathan for helping me to solve problems in FLUENT. Use of the resources at the Artic Region Supercomputing Center to run this software is acknowledged.

Last but not least, I wish to record my sincere appreciation and thanks to my parents, family and friends for their invaluable support, patience and encouragement throughout.

Dedication

To my beloved *Brother Late Mr. Gajanan Juvekar*
for his love, compassion and sacrifice

CHAPTER ONE

INTRODUCTION

Due to rapid developments in the electronic industry, including dramatic increase in chip densities and power densities, as well as continuous decrease in physical dimensions of electronic packages, thermal management is, and will continue to be, one of the most critical areas in electronic product development. It will have a significant impact on the cost, overall design, reliability and performance of the next generation microelectronic devices.

The Center for Nanosensor Technology at the University of Alaska Fairbanks is concentrating on developing a program in advanced technology for microelectronic devices. The goal under this program is research and development of multiple classes of microsensors. In recent years, as the microprocessors in electronic devices are miniaturized, their thermal management has become harder necessitating innovative designs. The new generation high performance microprocessors will generate large amounts of heat within a smaller surface area and will require proper heat sink design to cool them. Now- a- days the standard approach for electronics cooling is fan-cooled heat sinks. Therefore, we have started our research with developing thermal models for forced convection heat sinks.

The ultimate goal of this project is to come up with efficient cooling models for microelectro-mechanical devices and in future to extend it to nanoscale devices. To benchmark our thermal and fluid dynamics models, we chose the Intel Pentium III microprocessor having specifications of 866 MHz, 133 MHz system bus frequency (Intel,2001) for forced convection cooling and Intel Pentium II processor with 333 MHz for natural convection cooling. These widely used chips were adopted by us to develop heat transfer and fluid dynamics equations for cooling of electronic equipment. We applied the equations to designed heat sinks for electronic processors to test the accuracy of our model equations. Then we designed microscale heat sinks. The objective was to

optimize heat dissipation and achieve proper thermal management of electronic devices by maintaining the chips at desirable temperatures. With the results of this thermal model predicting similar heat dissipation values as reported by the manufacturer, we adopted our model as the guideline for future designs. In the next step, we simulated a two-dimensional model using a computational fluid dynamics (CFD) code, Fluent. After refining various numerical parameters the predicted heat dissipation rates were in good accord with the actual heat dissipation rates specified by manufacturers. Then we miniaturized the processor chip size to micrometer scale and designed heat sinks based upon the models we had developed. Mathematical equations for natural convection heat sinks with high emissivity paint were also developed in the later part of this study.

As the heat flux value to be dissipated keeps on rising (about 150 W/cm^2 or more) with new demands for micro to nano sensors, it is envisioned that we may need to go to more efficient modes of electronics cooling such as liquid spray cooling and cooling through micro-channels. Heat-pipes are already used in laptop computers and future advancements are necessary to apply them as micro heat pipes in micro scale processors.

For our cases we studied pure conductive and convective cooling. We investigated only heat sinks as cooling technique for processor chips. The higher the density of electronic parts, e.g transistors inside a processor, the higher will be the heat generated per unit area. There are two paths to dissipate this generated heat. The first path for heat flow is from the processor to the printed circuit board via leads and interconnects. Ju & Goodson (1999) claim that as the dimensions of interconnects decreases the resultant changes in current density make them more susceptible to failure during electrical stresses. To dissipate heat along this path, heat spreaders made up of high thermal conductivity materials like copper are being used these days. Then heat will flow from the chip to the heat spreader and to the printed circuit board. But as we are interested in analyzing the heat sink as the cooling device we know that the heat conduction to the printed circuit board is small. This heat conduction to the PCB will be discussed in section 3.2.1. The second path for heat flow is mainly from the processor to

the thermal adhesive and then to the heat sink and finally to the environment either by forced or natural convection.

For this heat flow path, there is conduction from the processor to the adhesive and to the base of the heat sink, so we will study this heat conduction and estimate the temperature of the base of heat sink. Another important analysis is the transient heat conduction to evaluate steady state temperatures for longer operational times of the processor and figure out the time to reach these temperatures. After finding out the base temperature of heat sink we used extended surface analyses. Kraus (1982) gives a good description of these extended surfaces and presents a detailed analysis for such surfaces having different geometries. We are using rectangular fins with constant cross sectional area for our analyses.

For convection cooling (i.e., natural and forced), we used different empirical correlations to find the heat transfer coefficient and ultimately the heat loss by the fins for such cases. To verify these analytical results, we used Fluent as the CFD code. In this code we were interested mainly in visualizing the velocity pattern, Nusselt number, and heat transfer coefficient. After finding the heat loss from all fins we compared the analytical and numerical results. The results were found to be in close agreement with the analytical results and we tried to adopt a similar model for a miniaturized microprocessor chip. To realize this, we first scaled down the heat sink dimensions on the basis of chip geometry.

As we miniaturized our sink, the first question was whether we could apply these available correlations to flow in microchannels? Carlen and Mastrangelo (2002) present a gas model to validate equations based on continuum theory for microflows. They used the Knudsen number, a characterization parameter, which is the ratio of characteristic length of the microchannel to the mean free path of a gas molecule. According to the range of the Knudsen number they classified three types of flow i.e. laminar, transition and molecular. If we are in the laminar region then we can apply our existing conventional correlations to find the heat loss from fins.

A lot of attention is being devoted to frame equations and correlations for microchannel flows. Beskok and Karniadakis (1999) present a lucid yet clear analysis of flow in micro channels and have worked at developing a model for rarified gas flows in channels, pipes and ducts for a wide range of Knudsen numbers. They also present a new boundary condition that accounts for the increased surface-fluid interaction and checked its validity.

Sabry (2000) asserts that, as the size of microchannel reduces, the fluid flow and heat transfer characteristics deviate from those resulting from continuum theory. Many hypotheses were advanced to explain some of these deviations but they were usually found to be in contradiction with observed results. Hence no authoritative conclusions have been given so far for explaining this phenomenon. He also mentions in his paper that a new hypothesis will be advanced based upon the increased role of surface roughness on flow and heat transfer in microchannels.

In many studies like calculating the lift and drag on Micro Electro Mechanical Systems (MEMS), the first attempt is always to check the flow regime. At the MEMS scale the “no slip” condition is replaced by a slip flow condition and is presented by Martin, Kurabayashi, Boyd (2001). Basically this depends on the Knudsen number.

There is no dearth of textbooks that deal with thermal management of relatively “macro” electronic systems (e.g. Tummala, 2001) but quality textbooks on microelectronics thermal management are just emerging. One such text worth mentioning is by Yeh and Chu (2002). The authors explain different cooling techniques proposed for micro size equipment and also the technical challenges associated with some of them. The most promising cooling techniques for the next generation processors, namely, two-phase cooling, thermoelectric cooling, etc. are discussed in reasonable depth.

CHAPTER TWO

THEORY

2.1 Heat Conduction in Chips and Substrates

While analyzing the thermal aspect of electronic devices, heat conduction plays an important role. Heat flux in a given direction is proportional to the gradient of temperature in that direction and is positive in the direction of decreasing temperature. If the temperatures of surfaces are T_1 and T_2 , then total heat transfer rate q across a cross sectional area A is given by the Fourier's Law of heat conduction.

$$q = k A (T_1 - T_2) / L \quad (2.1)$$

where L is the thickness of the slab and k is the thermal conductivity of the material.

2.2 Temperature Distribution in a Processor Chip Generating Heat

While the electronic device is running, the memory chip is generating heat due electrical energy flow. Assumptions of this theory are- steady state heat conduction, constant thermal properties, and rate of internal energy generation q''' is uniform and constant.

From an energy balance i.e.

$$\text{Net heat transfer rate} + \text{Rate of internal energy generation} = 0$$

From Fourier's Law for a solid with one dimensional temperature distribution, the governing equation is given by (Suryanarayana, 1995)

$$\frac{d^2 T}{dx^2} + \frac{q'''}{k} = 0 \quad (2.2)$$

and the general solution for the above governing equation is given by

$$T = -\frac{q''' x^2}{2k} + c_1 x + c_2 \quad (2.3)$$

The constants c_1 and c_2 are obtained by applying different boundary conditions.

2.3 Transient Heat Conduction in the Chip and the Heat Sink

Lumped Analysis:

The temperature of a body depends on both time and spatial coordinates. If the Biot number ($Bi = ht / k$) is small i.e. $Bi < 0.1$, the approximation of spatially uniform temperature at any given instant gives acceptable results. We have conductive resistances for silicon chip, interface bond and base of the aluminum heat sink. Also we have convective resistance for fins. Biot number is the ratio of sum of the conductive resistances to convective resistance. Conductive resistance for any material is given by

$$R = (L / kA) \quad (2.4)$$

where L is the characteristic length, k is the thermal conductivity of the material and A is the cross sectional area. If a component is energized with a heat generation q_G in watts, then the heat entering and heat leaving from the component satisfy the energy balance equation. Heat leaving from the component is given by

$$q = q_G - K_e (T - T_0) \quad (2.5)$$

where K_e is conductance due to conduction and convection to the environment at temperature T_0 and T is the lumped temperature of the whole body. Increase in the internal energy ΔE is given by

$$\Delta E = Mc_p dT/dt \quad (2.6)$$

where M is the mass of the components.

The differential equation from energy balance to be solved is (Kraus, Bar-Kohen, 1983)

$$q_G - K_e (T - T_0) = Mc_p dT/dt$$

After solving this differential equation, lumped temperature $T(t)$ of the solid at time 't' is given by

$$T(t) = T_0 + \frac{q_G}{K_e} (1 - e^{-(K_e / Mc_p)t}) \quad (2.7)$$

Steady state temperature of the body can be found by substituting time to be infinity. This equation is based upon lumped analysis.

2.4 Interface/Contact Resistance

The heat generating chip is generally connected to a heat sink to cool it as we observe in personal computers. There exists an interface between the chip and the heat sink, which presents a contact resistance. For perfectly adhering solids, geometrical differences in crystal structure (lattice mismatch) can impede the flow of phonons and electrons across the interface. This resistance is known as interface resistance.

When two materials are in contact with each other, because of roughness of interfaces the material is actually in contact with each other at very few places. There are some voids, which are usually filled with the fluid surrounding the material, which provides parallel path for the heat transfer. As this resistance is confined to very small region, there is sharp change in temperature across the boundaries of interface materials. This interface resistance depends on surface finish, mounting pressures, flatness, contact area, material type and most importantly, the thickness of the bond material.

The contact resistance is given by (Suryanarayana, 1995)

$$R_c'' = \Delta T / q'' \quad (2.8)$$

Where ΔT is temperature drop across the interface (K) and q'' is the heat flux across the interface.

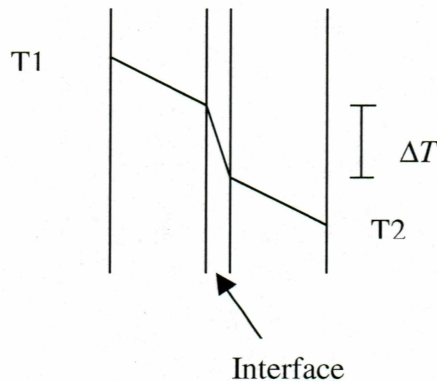


Figure 2.1 Schematic to represent contact resistance.

2.5 Spreading Resistance

In chip packages heat spreaders are provided for lateral spreading of heat generated in chip. These increase the cross sectional area for heat flow. But there is an additional resistance associated with this lateral flow of heat known as spreading resistance.

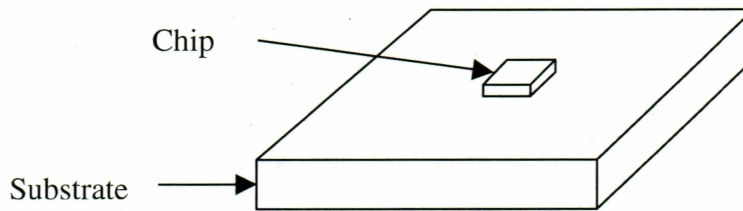


Figure 2.2 Schematic of the chip placement on a substrate.

The spreading resistance for a small heat source on a thick substrate / spreader is given by (Kraus, Bar-Cohen, 1995)

$$R_{sp} = \frac{1 - 1.41\epsilon_1 + 0.344\epsilon_1^3 + 0.043\epsilon_1^5 + 0.034\epsilon_1^7}{4ka} \quad [\text{K/W}] \quad (2.9)$$

where ϵ_1 is the ratio of heat source area to the substrate area and a is the square root of the area of the heat source and k is the thermal conductivity of the substrate.

2.6 Heat Transfer via Convection from the Heat Sink

In convection, heat loss from a surface is given by

$$q = h A (T_s - T_f) \quad (2.10)$$

where subscripts 's' and 'f' denote surface and fluid respectively, and h is the convective heat transfer coefficient. Cooling of components can be achieved by forced or natural convection.

2.6.1 Forced Convection

In forced convection, the heat transfer coefficient h is a function of Nusselt number, Reynolds number and Prandtl number. Reynolds number is a function of the fluid properties like density of the fluid, characteristic geometry and viscosity of the fluid. It is given by

$$Re_L = \frac{\rho U_\infty L}{\mu} \quad (2.11)$$

where 'L' is the dimensional characteristic length.

Prandtl number is given by

$$Pr = \frac{C_p \mu}{k} = \frac{\nu}{\alpha} \quad (2.12)$$

where ν is the kinematic viscosity of fluid (m^2/s) and α is thermal diffusivity of fluid (m^2/s). For fluid flow over a flat plate the flow is generally considered to be boundary layer type of flow. For such cases, when $Re_L < Re_{cr}$ where critical Reynolds number is 5×10^5 , the flow regime is considered as laminar. The Nusselt number for this laminar boundary layer is given by (Suryanarayana, 1995)

$$Nu_L = 0.664 Re_L^{1/2} Pr^{1/3} \quad (2.13)$$

This Nusselt number is based on average heat transfer coefficient over length L . The heat transfer coefficient is found to be

$$h = \frac{Nu_L k}{L} \quad (2.14)$$

2.6.2 Natural Convection Analysis

In natural convection the motion of fluid is mainly due to the temperature difference between the adjacent fluid and the surface. This causes changes in body force,

which makes natural convection occur. In natural convection the Nusselt number is a function of the Rayleigh number and Prandtl number. Rayleigh number is product of the Grashof number and Prandtl number. Different correlations are available in literature.

The Nusselt number for vertical plates and for low Rayleigh number with uniform wall temperature is given by (Suryanarayana, 1995)

$$Nu_L = 0.68 + \frac{0.67 Ra_L^{1/4}}{[1 + (0.492 / Pr)^{9/16}]^{4/9}} \text{ for range } 10^{-1} < Ra_L < 10^9 \quad (2.15)$$

$$Nu_L = \{0.825 + \frac{0.387 Ra_L^{1/6}}{[1 + (0.492 / Pr)^{9/16}]^{8/27}}\}^2 \text{ for range } 10^{-1} < Ra_L < 10^{12} \quad (2.16)$$

The lower limit of 10^{-1} for Ra_L is based on experiments done by Churchill and Chu. If $Ra_L < 10^9$ then Equation (2.13) gives the better results.

Nusselt number for vertical plates with uniform heat flux is given by (Suryanarayana, 1995)

$$Nu_L = 0.68 + \frac{0.67 Ra_L^{1/4}}{[1 + (0.437 / Pr)^{9/16}]^{4/9}} \quad Ra_L < 10^9 \quad (2.17)$$

$$Nu_L = \{0.825 + \frac{0.387 Ra_L^{1/6}}{[1 + (0.437 / Pr)^{9/16}]^{8/27}}\}^2 \quad 10^{-1} < Ra_L < 10^{12} \quad (2.18)$$

2.7 Heat Transfer from the Fins of a Heat Sink

Increasing surface area decreases the thermal resistance, which leads to the concept of using fins to augment heat transfer. Heat is conducted to the surface of fins from the heat source. This surface is exposed to the fluid having ambient temperature T_∞ . Then this heat is convected to the environment.

The governing equation for a fin is obtained by an energy balance, i.e. whatever heat is conducted to the surface is convected to the environment. The final form of governing equation is given by (Suryanarayana, 1995)

$$\frac{d^2\theta}{dx^2} - m^2\theta = 0 \quad (2.19)$$

where we define $\theta = T - T_\infty$ and $m^2 = \frac{hp}{kA}$

The general solution of the above differential equation leads to the heat loss from the fins via the following expression

$$q = \sqrt{hPAk} \theta_b \frac{\sinh(mL) + (h/km) \cosh(mL)}{\cosh(mL) + (h/km) \sinh(mL)} \quad (2.20)$$

$\theta_b = T_b - T_\infty$, where T_b is base temperature.

For the type of longitudinal fins of constant cross-sectional area used in the heat sink that we are analyzing, the temperature of tip of the fin is given by

$$\frac{\theta_t}{\theta_b} = \frac{1}{\cosh(mL) + \left(\frac{h}{km}\right) \sinh(mL)} \quad (2.21)$$

$\theta_t = T_t - T_\infty$, where T_t is tip temperature.

2.8 Radiation Heat Transfer from Heat Sinks

Radiation generally plays a minor role in heat transfer when forced convection dominates the cooling mode of the heat sink. However, it may play a major role when the fins of the heat sink are cooled by natural convection. The heat loss from the fin surfaces of a heat sink by radiation is given by (Suryanarayana, 1995)

$$q = \sigma A F_{1-2} \epsilon (T_s^4 - T_\infty^4) \quad (2.22)$$

where σ is Stefan Boltzman's constant ($5.67 \times 10^{-8} \text{ W/m}^2\text{K}^4$), F_{1-2} is view factor and ϵ is the emissivity of the material. Radiation between two bodies depends on how these objects see each other. F_{1-2} is defined as the ratio of radiant energy leaving surface 1 and

reaching 2, to the total radiant energy leaving surface 1. In the case of flat longitudinal fins separated by an air gap, view factor for identical, aligned rectangles directly opposite to each other is given by (Suryanarayana, 1995)

$$F_{1-2} = \frac{2}{\pi xy} \left\{ \ln \left[\frac{(1+x^2)(1+y^2)}{1+x^2+y^2} \right]^{1/2} + x(1+y^2)^{1/2} \tan^{-1} \left[\frac{x}{(1+y^2)^{1/2}} \right] \right. \\ \left. + y(1+x^2)^{1/2} \tan^{-1} \left[\frac{y}{(1+x^2)^{1/2}} \right] - x \tan^{-1} x - y \tan^{-1} y \right\} \quad (2.23)$$

$x = L/D$ and $Y = L/D$ where L is the length and D is the gap between fin surfaces.

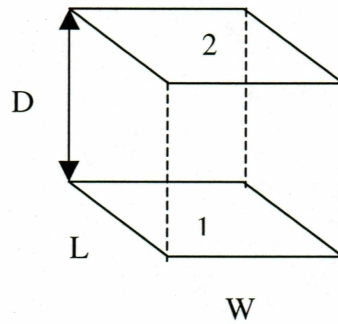


Figure 2.3 Schematic of dimensions of fins facing each other for view factor determination

If the surface i and surface k with different areas share a common edge, then the view factor correlation is given by reciprocal law. (Suryanarayana, 1995)

$$A_i F_{i-k} = A_k F_{k-i} \quad (2.24)$$

Another important correlation is sum of the view factors from a single surface is always equal to 1.

$$\sum_{k=1}^N F_{i-k} = 1 \quad (2.25)$$

Further details of radiation view factor between the fin surfaces and their surroundings are presented in Section 3.5.

CHAPTER THREE

ANALYTICAL SOLUTIONS FOR MACRO SCALE CHIP

The ultimate goal of this project is to come up with efficient heat dissipation models for micro-electro-mechanical devices and in future to extend it to nanoscale devices. To start with and to build a model case, we chose the Intel Pentium III microprocessor having specifications of 866 MHz, with a 133 MHz system bus frequency. This chip is commonly used in personal computers. Hence we adopted it to develop heat transfer and fluid dynamics equations for cooling of electronic equipment. The manufacturers of this equipment desire to dissipate the heat generated in microprocessor efficiently. By dissipating this heat the chips can be maintained at lower temperatures. Operation of chips at lower temperature ensures longer life. With results of this thermal model predicting similar heat dissipation values as reported by the manufacturer, we will adopt our model as the guideline for future designs. In the next step, we will attempt a more complex simulation using the finite element fluid dynamics code, Fluent, to design the heat sink. After refining the predicted heat dissipation to agree very closely with actual heat dissipation presented by manufacturers, we will miniaturize the processor chip size to micrometer scale and design heat sinks, based upon the models we have developed. Mathematical expressions for natural convection heat sinks with high emissivity paint will also be developed. For convection analysis we will refine the present computation by the computer code Fluent.

As the heat flux value to be dissipated keeps on rising (about 150 W/cm^2 or more) with new demands for micro to nano sensors, it is envisioned that we may need to go to more efficient modes of electronics cooling such as liquid cooling through micro-channels and adoption of micro heat-pipes.

3.1 Model Description

The thermal specifications and design considerations of the microprocessor were obtained from the Intel Pentium data sheet (Intel, 2001).

Specifications

- 1) Thermal Design Power (TDP) represents the maximum amount of heat the device is required to dissipate and for the chip we have selected, it is specified as 23 W by Intel.
- 2) The heat sink should be designed to dissipate the TDP power without exceeding the maximum junction temperature T_j . The junction temperature is defined as the maximum temperature occurring on the top surface of the chip. Usually it is at the geometric center of the chip on the surface. In case of Pentium III, Intel recommends this temperature to be 80 Deg C.
- 3) The heat sink should be designed considering the fact that temperature of case, T_{case} should not exceed that 69 Deg C. Case temperature is defined as the average temperature of the encapsulant surrounding the chip.
- 4) Dimensions of chip are 11mm X 9mm X 1mm.

For simplicity, it is assumed that the chip is made up of silicon having a thermal conductivity of 148 W/mK. (Fabis, Windischmann, 2000). There are metallic components, e.g. transistors, diodes etc. within the chip. However, it is difficult to get this information from manufacturers. Therefore, for approximate thermal modeling purposes, many analysts treat it simply as a silicon material. The heat sink is made up of pure aluminum having specific heat of 900 J/kgK and thermal conductivity of 240 W/mK (Suryanarayana, 1995).

This processor is directly cooled with a fan heat sink. The processor fan heat sink is able to keep the processor core within the specifications mentioned above when

installed in a chassis that provides good thermal management. The dimensions of this fan-cooled heat sink are given below. Note that all dimensions mentioned here are in inches.

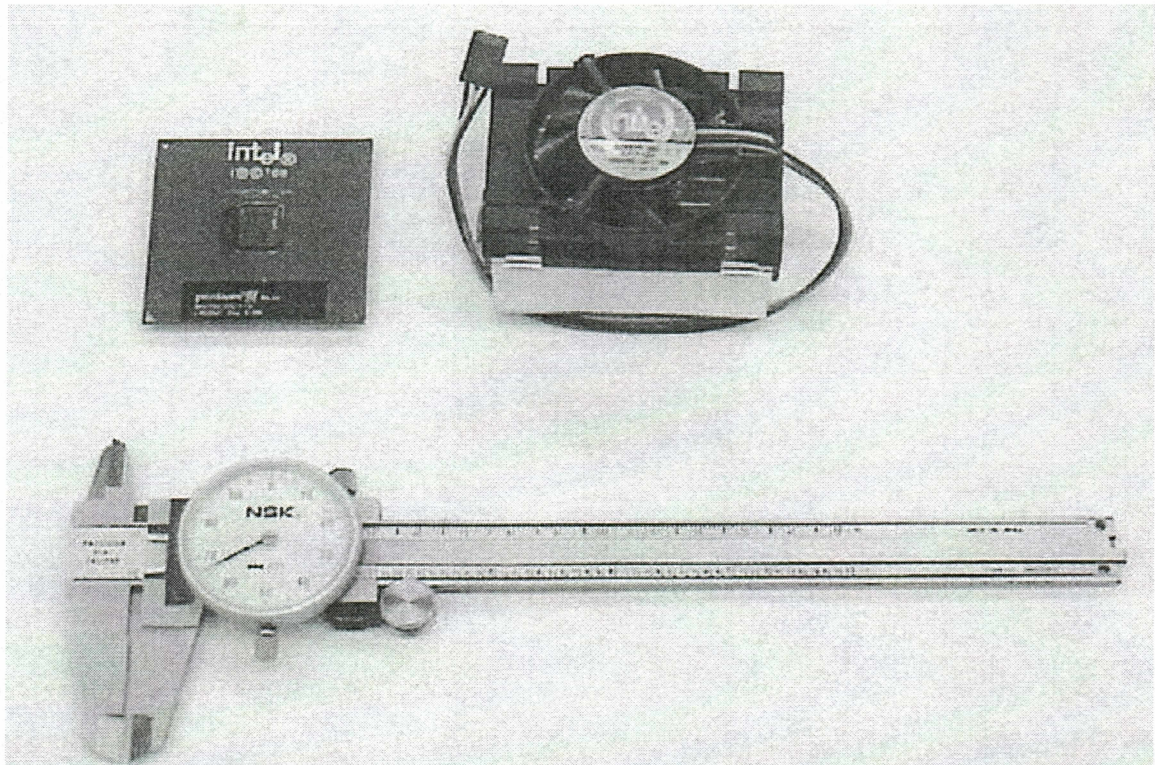


Figure 3.1(a) Layout of Pentium III chip with heat sink and fan assembly.

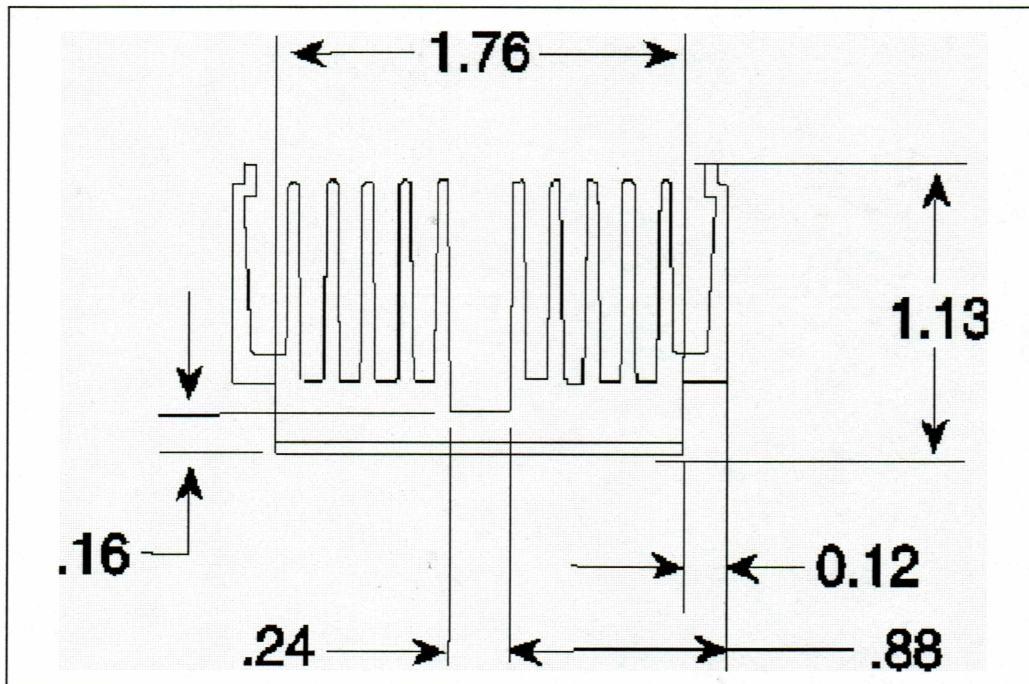


Figure 3.1(b) Important dimensions of the heat sink geometry.

3.2 Conduction Analysis

3.2.1 Heat Conduction to the Printed Circuit Board (PCB)

From the layout for Pentium III chip as given by Intel, we can see that the die surface is mounted on the substrate with the help of underfill material. The schematic of this layout is shown in Figure 3.2.

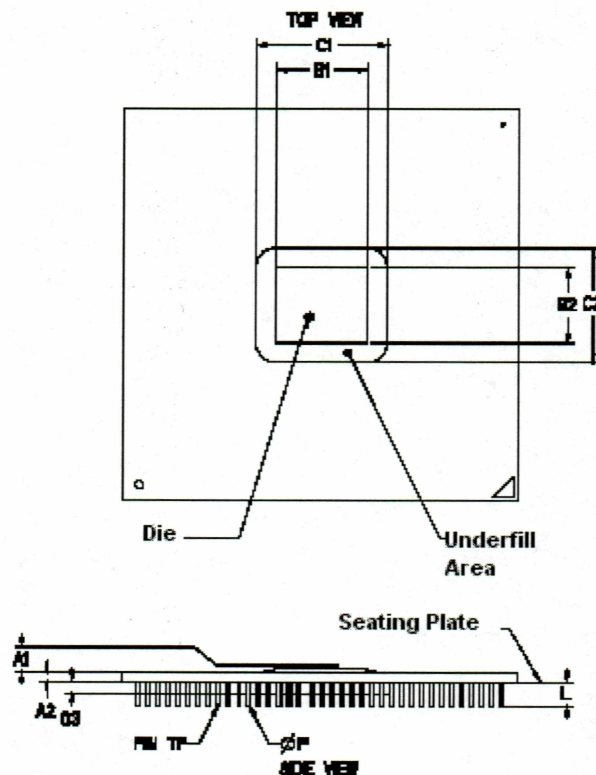


Figure 3.2 Schematic of die placement over the substrate with underfill.

All the dimensions in the Figure 3.2 are obtained from Intel Datasheet (Intel, 2001).

Maximum dimensions for underfill area are, $C1 = 23.5$ mm, $C2 = 21.6$ mm and height $A1 = 0.89$ mm. Generally underfill material used for such cases is epoxy with thermal conductivity of 0.2 W/mK (Tessera Tech. Inc, 2003). From Equation (2.1), the heat loss to the PCB from the die is calculated to be 3.9 W, which is 17% of the total heat generated by the die. However, while designing the heat sink in the subsequent sections, we have considered the total heat generated to be dissipated by convection and radiation from the sink. The heat conduction to the PCB plays a very small part.

3.2.2 Temperature Distribution in the Chip from Heat Generation Theory

From the Intel data sheet we found another limitation that the case temperature of chip should not exceed 69 Deg C. Case temperature is the temperature of outermost

surface of chip. The surface touching the sink should have maximum heat transfer. The available boundary condition for the side facing the printed circuit board (PCB) should be at 69 Deg C. The second boundary condition is a known heat flux from continuous generation of heat of 23 Watts that flows through the other face of chip to the heat sink.

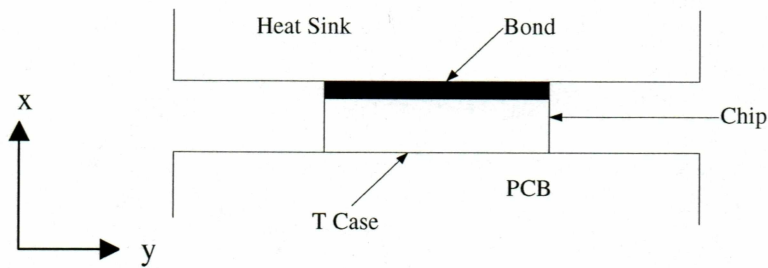


Figure 3.3 Schematic diagram of chip placement.

The Fourier equation with heat generation is given by equation (2.2), where

$$q''' = Q/V = 0.2323 * 10^9 \text{ W / m}^3 \quad (3.1)$$

Integrating Equation (2.2) twice and applying the two boundary conditions of known heat flux of 23 W uniformly and case temperature of 69 Deg C at the bottom, we obtain the final equation for temperature distribution in the chip, where x is the distance measured from the center.

$$T = \frac{-q'''}{2k} x^2 - 783 * x + 68.805 \quad (3.2)$$

Equation (3.2) is plotted showing the temperature profile in the chip in Figure 3.4

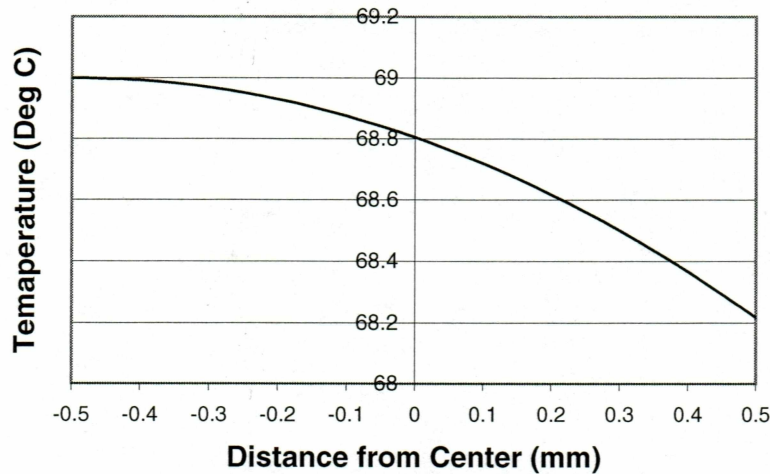


Figure 3.4 Temperature profile in the processor chip.

From the plot it is seen that temperature of the top surface (+ side) of the chip is about 68.2 Deg C whereas temperature at bottom surface is held constant at 69 Deg C.

3.2.3 Interface Resistance with a Bond Material

To have a very good contact between the chip surface and heat sink surface it is necessary to use a very good bonding material. Selection of bonding (interface) material is very crucial as it offers resistance to heat flow. This interface resistance depends on surface finish, mounting pressures, flatness, contact area, material type and most importantly, the thickness of the bond material. The resistance at the interface is confined to very small and thin region. So there will be change in temperature in this region. From Equation (2.8), using Aluminum Nitride as the bonding material having $K = 230 \text{ W/mK}$ (Bar-Cohen & Kraus, 1990) and an average thickness of 0.114 mm (Lee, 1995). We found the temperature drop across the bond is 0.12 Deg C. This is desirable, since efficient heat transfer demands a small resistance to heat flow from the chip to the heat sink. Materials used as bonding glues with respective thicknesses are given in a table 3.1. Columns 1,2 and 3 were obtained from Lee (1995) and we computed columns 4 & 5.

Table 3.1 Thermal Properties of Interface Materials

| Material | Conductivity W/m °C | Thickness m x 10 ⁵ | Resistance m ² C/W x 10 ⁻⁴ | Temperature at other face °C |
|---------------------------------|------------------------|----------------------------------|---|---------------------------------|
| Three O link Thermal cmp | 0.3937 | 5.08 | 1.29 | 68.197 |
| High Performance Thermal cmp | 1.181 | 5.08 | 0.43 | 68.199 |
| Kon Dux | 1.181 | 12.7 | 1.075 | 68.1975 |
| A Dux | 0.315 | 10.16 | 3.225 | 68.1925 |
| 1070 Ther A Grip | 0.5512 | 15.24 | 2.765 | 68.1936 |
| 1050 Therm A Grip | 0.3543 | 12.7 | 3.584 | 68.192 |
| 1080 Therm A Grip | 0.3937 | 5.08 | 1.29 | 68.197 |
| 1081 Therm A Grip | 0.748 | 12.7 | 1.6978 | 68.11 |
| A phi 220 @ 20 psi | 2.9134 | 50.8 | 1.744 | 68.196 |
| 1897 in Sil 8 | 0.3937 | 20.32 | 5.16 | 68.188 |
| 1898 in Sil 8 | 0.315 | 15.24 | 4.838 | 68.188 |

3.2.4 Spreading Resistance to the Substrate

When the chip as a heat source sits on a thick substrate or heat spreader, there is an additional thermal resistance due to lateral heat flow. To calculate spreading resistance we have to obtain ε_1 and 'a', where ε_1 is the ratio of the heat source area to the substrate area and 'a' is the square root of the heat source area. In our case, from equation (2.9)

$$\varepsilon_1 = 99/2250 = 0.044$$

$$\text{and } a = \sqrt{99} = 9.9 \text{ mm}$$

Aluminum is taken as the heat spreader. Hence the spreading resistance R_{sp} is 0.039 K/W. Spreading resistances exist whenever heat flows from one region to another in different cross sectional areas. In the case of heat sink applications, the spreading resistance occurs in the base-plate when a heat source of a smaller footprint area is mounted on a heat sink with a larger base-plate area. This results in a higher local temperature at the location where the heat source is placed. The smaller the heat source, the greater the spreading resistance, resulting in a greater temperature rise at the center.

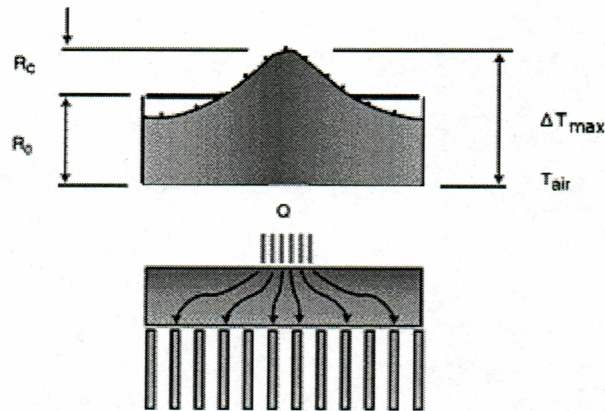


Figure 3.5 Two-dimensional schematic view of spreading resistance.

Another correlation is available to find spreading resistance (Lee, 1998).

$$R_c = \frac{\sqrt{A_p} \cdot \sqrt{A_s}}{k \sqrt{\pi A_p A_s}} \times \frac{\lambda K A_p R_o + \tanh(\lambda t)}{1 + \lambda K A_p R_o \tanh(\lambda t)} \quad (3.3)$$

$$\text{and } \lambda = \frac{\pi^{1/2}}{\sqrt{A_p}} + \frac{1}{\sqrt{A_s}}$$

where A_s is the contact area of the heat source; A_p is the area of the heat sink base-plate; t is the thickness of the heat sink base plate; R_o is the average heat sink thermal resistance.

In our case, $A_s = 99 \text{ mm}^2$, $A_p = 2250 \text{ mm}^2$, $t = 5 \text{ mm}$ and $k = 240 \text{ W/mK}$.

Hence $\lambda = 137.87 \text{ m}^{-1}$ from above substitutions. R_o is $1.6 \text{ }^\circ\text{C/W}$ from conduction calculations. The spreading resistance can be found to be $3.89 \times 10^{-3} \text{ }^\circ\text{C/W}$, which is negligible.

Hence, the maximum resistance, R_{total} is

$$R_{\text{total}} = R_o + R_c = 1.6 + 0.00389 = 1.60389 \text{ }^\circ\text{C/W}.$$

3.2.5 Steady State Heat Conduction in the Heat Sink Base

As shown in Figures 3.1 & 3.3, the processor chip that generates heat is attached to the aluminum heat sink by a bonding compound. Heat is conducted through this bonding layer into the base of the aluminum heat sink, which is 5 mm thick, and from there to the fins. The thermal analysis is based on one-dimensional steady state heat conduction, through this 5 mm thick base.

The input parameter for analysis is a heat flow of 23 W from side at $x=0$ at the bottom in Figure 3.1. The junction temperature may vary over a range. To determine the upper limit of heat flow, we first adopt a maximum junction temperature of 80 Deg C.

The base of the heat sink is treated as a slab of 5 mm thick i.e. $x=5$ mm. The dimension of heat sink is 45 mm X 50 mm.

According to the Fourier law of heat conduction, which is given by Equation (2.1) where Q is 23 W, which is conducted into the heat sink and is dissipated to the surroundings from the sink. From Equation (2.1), the temperature at $x=5$ mm i.e. at the other face of the base slab of the heat sink is 79.787 Deg C.

3.2.6 Transient Heat Conduction

When the microprocessor is not working, it is at room temperature. But whenever the power is switched ON, the microprocessor starts generating heat because of different resistors and diodes present in the circuit. After being switched ON, it will take some time for the chip to attain the steady state temperature. At steady state condition the amount of heat generated is the same as the amount dissipated. We are interested in finding how long does it take to reach steady state and what is that steady state temperature.

Lumped Analysis:

This analysis is dependant on the magnitude of Biot number. Biot number is the ratio of conductive to convective resistance. Usually Aluminum Nitride (AlN) is used as bond material between the sink and the chip. The thermal conductivity of AlN is about 230 W/mK. From Equation (2.4), the resistances for different materials are found to be

$$R_{si} = (L / k_{si}A) = (1 \times 10^{-3}) / (148 \times 99 \times 10^{-6}) = 0.068 \text{ } ^\circ\text{C/W} \quad (\text{Silicon})$$

$$R_{bond} = (L / k_{bond}A) = (1.143 \times 10^{-4}) / (230 \times 99 \times 10^{-6}) = 0.005 \text{ } ^\circ\text{C/W}$$

$$R_{Al} = (L / k_{Al}A) = (5 \times 10^{-3}) / (240 \times 2250 \times 10^{-6}) = 0.00926 \text{ } ^\circ\text{C/W} \quad (\text{Aluminum})$$

The convective resistance for the fin is given by equation (2.4)

$$R_{conv} = 1 / (hA)$$

The area available for convection is 0.02895 m^2 . From above equation, convective resistance is calculated with $h = 22.5 \text{ W/m}^2\text{K}$ obtained in Section 3.3.

$$R_{\text{conv}} = 1 / (22.7 \times 0.02895) = 1.521 \text{ } ^\circ\text{C/W}$$

The Biot number is given by

$$\text{Bi} = (R_{\text{si}} + R_{\text{bond}} + R_{\text{Al}}) / R_{\text{conv}} = 0.05$$

From above calculations we conclude that Bi in our case is much less than 0.1. Hence we can use lumped analysis to find out the temperature of the heat sink.

Kraus and Bar-Cohen (1983) presented the equations of transient heat conduction governed by an energy balance of the chip and sink. From Equation (2.7), we can find the steady state temperature varying with respect to time t . K_e is the conductance to the environment that consists of conduction as well as convection. It is calculated to be $0.62 \text{ W/ } ^\circ\text{C}$. There are four resistances associated with the system. The thermal circuit for the resistances is shown in Figure 3.6, where the cumulative resistance is $1.6 \text{ } ^\circ\text{C/W}$.

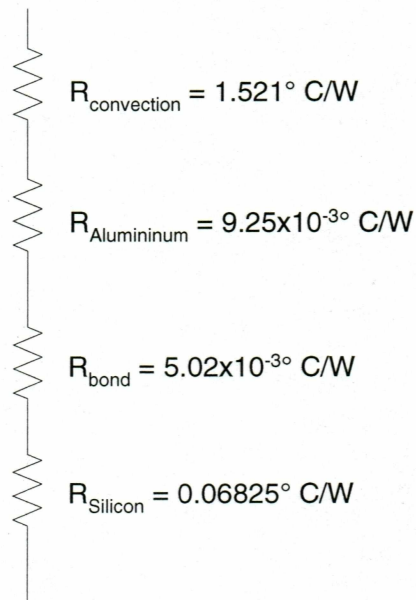


Figure 3.6 The heat flow network with different resistances.

Mass of the microprocessor chip is 0.21gms, which is calculated from dimensions of chip and density of silicon. For chip and sink system with aluminum, the total mass of the system is 180 grams (Intel, 2001). The temperature distribution of the whole system is shown in Figure 3.7.

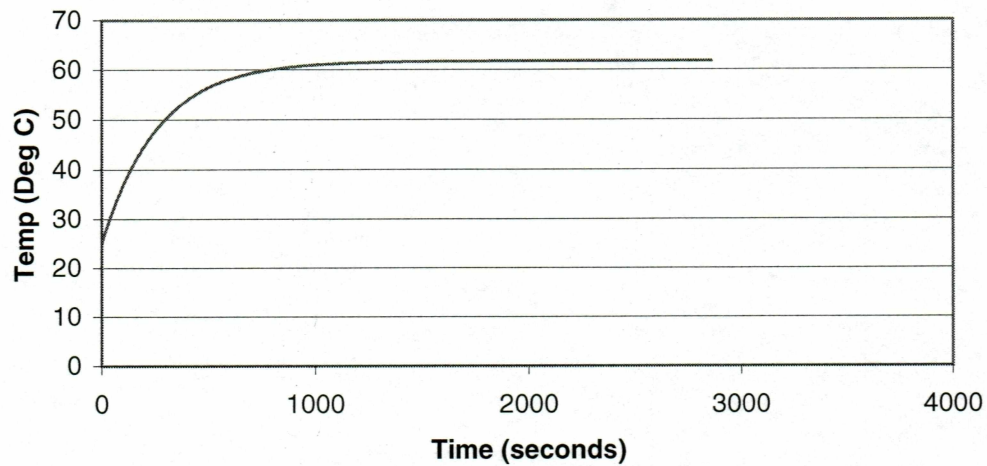


Figure 3.7 Temperature rise in chip and heat sink system until steady state is achieved.

From Figure 3.7 and our calculation it is observed that after 2860 seconds (47.67 minutes) the steady state temperature of 61.88 Deg C is achieved.

3.3 Convection Analysis

The cooling of chip is mainly accomplished by forced convection over the fins. For this processor chip a cooling fan is used. The airflow available from such type of fan is 10.2 CFM (Intel, 2001).

3.3.1 Calculation of Air Velocity

The ambient air is drawn in by the fan and blown over the fins. When the air flows on the fins, it is equally divided into two ways. So the available flow rate is 5.1 CFM because of symmetry. From Figure 3.1, we determine that the total available width for air to flow is 29.7 mm., and 15 mm is cumulative fin thickness for 10 fins. The schematic of airflow is shown in Figure 3.8.

The flow area available = 29.7 mm X 24.13 mm. = 716.661 mm²

Hence the velocity $U = \text{Vol. Flow} / \text{Area} = 3.3585 \text{ m/s}$.

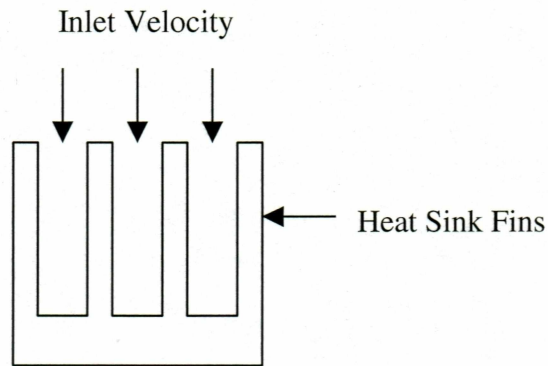


Figure 3.8 Schematic of airflow over the fins.

3.3.2 Reynolds Number

From Equation (2.11), Reynolds number is given by

$$\text{Re}_L = \frac{U_\infty L_1}{\nu} = 5341$$

for a flow over a characteristic length of 25 mm, because of splitting of flow. Based upon this Reynolds number the flow is in a laminar regime. For simplification, the turbulence generated by the fan is neglected.

3.3.3 Nusselt Number

For laminar flow over a flat surface, the correlation (2.13) is found to be applicable (Suryanarayana, 1995).

$$\text{Nu}_L = 0.664 (\text{Re}_L)^{1/2} (\text{Pr})^{1/3} = 43.33 \quad (3.3)$$

For air Prandtl number $\text{Pr} = 0.712$

3.3.4 Heat Transfer Coefficient

The relation between Nusselt number & heat transfer coefficient h is given by Equation (2.14)

$$h = \text{Nu}_L k_a / L_1$$

Substitution of various numbers yields

$$h = 22.7 \text{ W/m}^2 \text{ } ^\circ\text{C}$$

3.4 Heat Loss from Fins

The finned system analysis is based on energy balance. The differential equation obtained from (Suryanarayana, 1995) for fins is given by Equation (2.19)

For the type of longitudinal fins of constant cross-sectional area used in the heat sink that we are analyzing, the temperature of tip of fin is given by Equation (2.21)

The fin is exposed to the fluid, which is air at an ambient temperature of 25 Deg C. This can be refined by measuring actual air temperature by a thermocouple inside a computer. We illustrate here three cases of convection heat loss.

Case I

Use the maximum junction temperature of 80 Deg C., to get an upper bound of heat loss. Therefore from Equation (2.21), it is found that the temperature of tip is 76.22 Deg C. The heat loss from both surfaces of each fin is 8.66 Watts obtained using Equation (2.20) and from ten interior fins is 86.6 W.

Case II

Here we use the calculated chip surface temperature, the contact resistance and the conduction through the sink base to obtain the temperature at base of fin to be 68 Deg C. It has been assumed that all air passes through the gap between the fins. So total available area for air to pass is 2250 mm^2 . So the velocity of air comes out to be 2.14

m/s. Hence Reynold's number $Re_L=3403.3$, Nusselt's number $Nu_L=34.59$ and heat transfer coefficient h is $18.125 \text{ W/m}^2\text{ }^\circ\text{C}$. To get lower bound we adopt the fin to be exposed to ambient air at 45 Deg C (Intel, 2001), the temperature at the tip is found from Equation (2.21) to be 67 Deg C . And the heat lost from each fin will be 2.96 W .

Case III

To obtain another lower bound for heat loss, it is considered that the heat flows through sink base having area $(11 \times 9) \text{ mm}^2$ of the chip only, then the temperature at base of fin is calculated to be 63.38 Deg C . The temperature at tip of the fin becomes 62.6 Deg C from Equation (2.21). And in this case, the heat lost from each fin will be 2.37 W from Equation (2.20).

3.4.1 Convection Results

Convection results for three cases as a parametric study is tabulated below.

Table 3.2 Comparison of convection heat losses for various cases.

| Case Number | Temp at Interface T_j C | Velocity U m/s | Reynold's Number Re | Heat Transfer Coefficient h w/mC | Temp of Fin Tip T_f C | Total Heat Loss for 10 fins Q Watts |
|------------------|---------------------------|----------------|---------------------|----------------------------------|-------------------------|-------------------------------------|
| 1 | 80 | 3.3585 | 5341.126 | 22.705 | 76.22 | 43.3 |
| 2 Area 45x50mm | 68.22 | 2.14 | 3403.3 | 18.125 | 67 | 14.8 |
| 3 Area 11 x 9 mm | 68.22 | 2.14 | 3403.3 | 18.125 | 62.5786 | 11.9 |

All above calculations are based on, airflow over 50 mm length.

Case 1 represents upper limit of heat transfer based on the flow-area (716.66 mm^2) of side openings & maximum interface temperature of 80 Deg C.

Case 2 represents lower limit of Heat Transfer based on available flow-area (2250 mm^2) from the top & maximum case temperature of 69 Deg C

Case 3 represents total available area of Heat Conduction is 99 mm^2 & maximum case temperature of 69 Deg C

3.5 Radiation Analysis

For electronic devices operating at low temperatures, radiation plays a minor role in heat dissipation from fins. Convection and radiation from heat sinks coexist, and when natural convection is the primary cooling mode, the contribution due to radiational cooling may become substantial. Also having high emissivity of heat sink surfaces, can significantly improve radiational heat transfer.

The heat loss due to radiation is given by

$$q = A\epsilon\sigma F_{1-2}(T_s^4 - T_\infty^4) \quad (3.4)$$

Considering the geometry of the fins on the heat sink, radiation will take place from the tip area, both side surface areas and from the base area. The tip will radiate heat to the surroundings with a full view factor ($F_A=1$). But the base and side surfaces are restricted because of close spacing of fins. The side surfaces of fins will radiate a fraction given by a view factor.

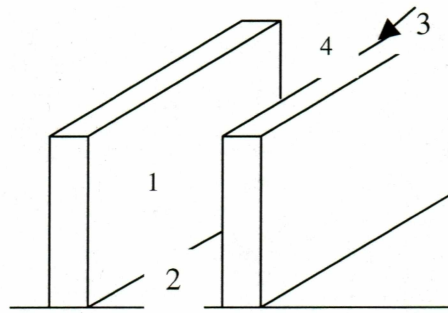


Figure 3.9 Schematic of channel surfaces for radiation.

From Figure 3.9, we can that face 1 will radiate to faces 2,3 and 4. To find the view factor F_{1-3} we can use relation for identical, aligned rectangles directly opposite to each other is given by Equation (2.23)

$$F_{1-3} = \frac{2}{\pi xy} \left\{ \ln \left[\frac{(1+x^2)(1+y^2)}{1+x^2+y^2} \right]^{1/2} + x(1+y^2)^{1/2} \tan^{-1} \left[\frac{x}{(1+y^2)^{1/2}} \right] \right. \\ \left. + y(1+x^2)^{1/2} \tan^{-1} \left[\frac{y}{(1+x^2)^{1/2}} \right] - x \tan^{-1} x - y \tan^{-1} y \right\} = 0.866$$

Referring to Figure 2.3, $x = L/D = 50/2.5 = 20$

$$y = W/D = 24.13/2.5 = 9.65$$

Emissivity of polished heat sink aluminum is 0.07.

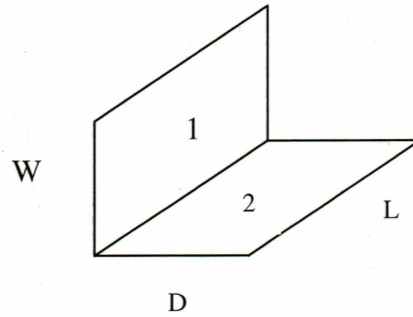


Figure 3.10 Schematic to find view factor for two rectangular surfaces sharing a common side.

For cases as shown in Figure 3.10, view factor, $F_{2-1} = 0.46$ (Suryanarayana, 1995)

From the reciprocal equation given by Suryanarayana, 1995,

$$A_i F_{i-k} = A_k F_{k-i} \quad \text{or} \quad A_2 F_{2-1} = A_1 F_{1-2} \quad (3.5)$$

Hence using Equation (3.5), we calculated view factor from the face to the base to be $F_{1-2} = 0.046$.

Suryanarayana, 1995, gives summation relation for an enclosure with N surfaces.

$$\sum_{k=1}^N F_{i-k} = 1; \quad \text{In our case } F_{1-2} + F_{1-3} + F_{1-4} = 1 \quad (3.6)$$

From Equation (3.6) we calculated the view factor for the face 1 and air at the top 4, and it is $F_{1-4} = 0.088$.

Here we consider two cases based on two different temperatures.

Case I: Tip Temperature of 352.18 K, Base temperature of 352.8 K. The ambient air temperature is 318 K. There are 12 fins having tip area of 75 mm^2 each, 22 faces of view

factor 0.088 and 2 faces with view factor of 1 of area 1206.5 mm^2 each, total base area available for radiation is 1485 mm^2 with view factor of 0.08 and 24 sides of fins having area of 36.195 mm^2 each with view factor of 1. The heat lost from 12 fins tip area is 0.0184 W, from 24 faces heat loss will be 0.098 W, from side area of fins 0.018 W and from base area 0.002 W. View factors for different faces are tabulated as follows

Table 3.3 View factor for various faces

| Faces | Area (mm ²) | View Factor |
|---------------|-------------------------|-------------|
| Faces of fins | 1206.5 | 0.088 |
| Base | 1485 | 0.08 |
| Sides of fins | 36.195 | 1.0 |

So the cumulative radiation will be 0.137 W and the distribution is shown in Figure 3.11.

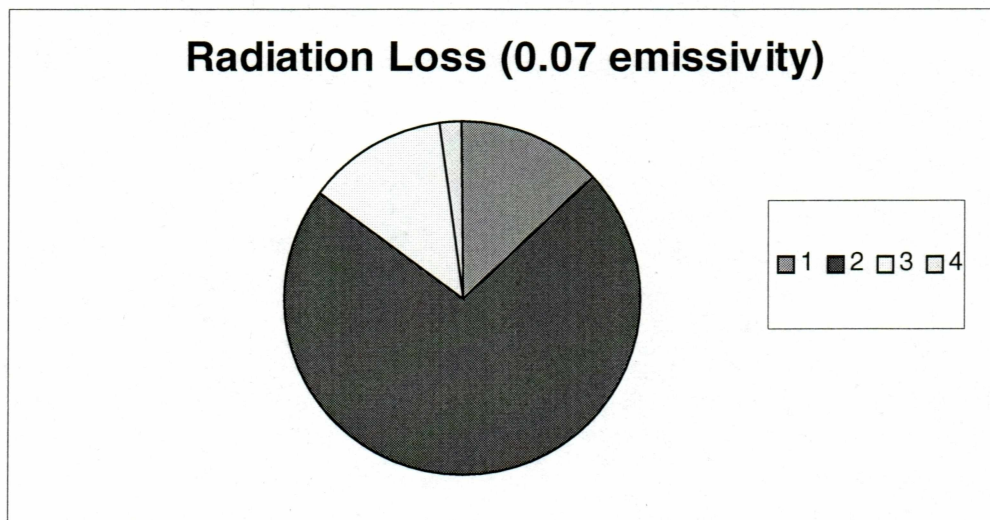


Figure 3.11 Distribution of radiation loss.

Notes: 1 : Radiation heat loss from Tip of Fins
 2 : Radiation heat loss from Face of Fins
 3 : Radiation heat Loss from Side of Fins
 4 : Radiation heat loss from Base Area.

3.5.1 Effect of Different Emissivity

One can increase the radiative loss by improving the emissivity of surface by applying proper paints. This is normally done for the heat sinks utilizing natural convection cooling. Different materials with varying emissivities is depicted in Table 3.4 (www.electro-optical.com)

Table 3.4 Materials with high emissivity used in Electronic industry

| Material | Emissivity |
|----------------------------|------------|
| Anodize Black | 0.88 |
| Lampblack Carbon | 0.84 |
| Carbon Black Paint NS-7 | 0.88 |
| Catalac Black Paint | 0.88 |
| Chemglaze Black Paint Z306 | 0.91 |
| GSFC Black Silicate MS-94 | 0.89 |
| Martin Black Paint N-15O-1 | 0.94 |
| Martin Black Velvet Paint | 0.94 |
| 3M Black Velvet Paint | 0.91 |
| Parsons black paint | 0.91 |

Therefore, the emissivity of extended surface was varied from 0.05 to 0.98 and the heat loss from radiation is depicted in Figure 3.12.

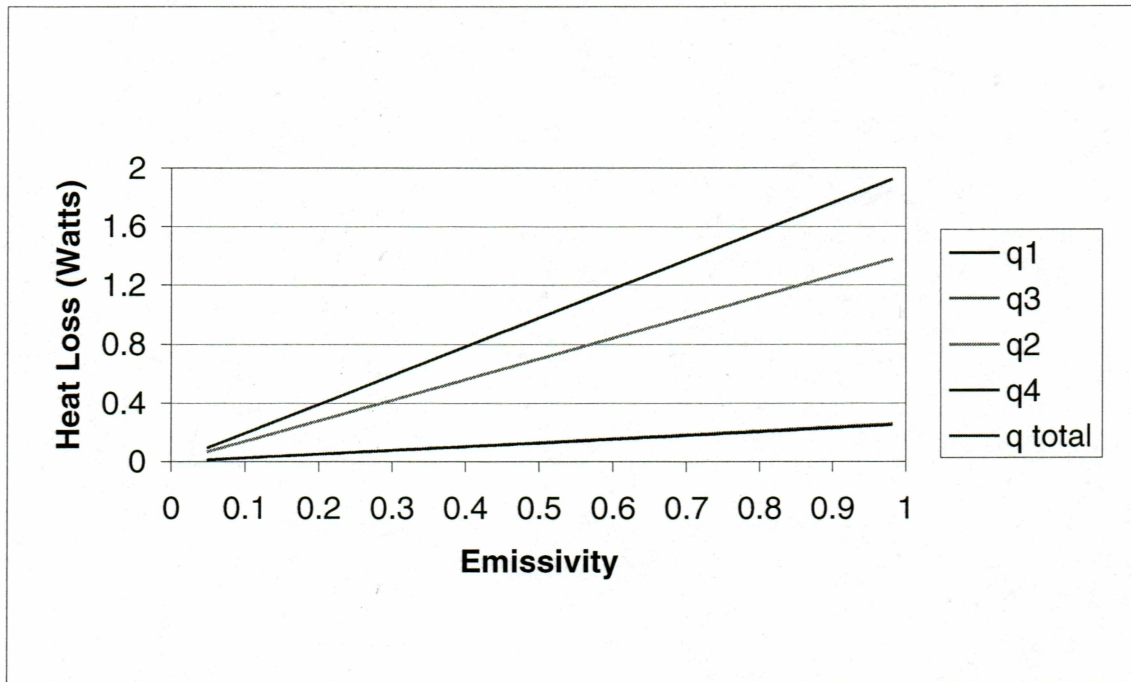


Figure 3.12 Effect of different emissivities.

Notes : q1 : Heat loss from tip of 12 fins

q2 : Heat loss from 24 faces of 12 fins

q3 : Heat loss from sides of 2 fins

q4 : Heat loss from base area

(q1,q3,q4 are small & indistinguishable)

Case II: Tip Temperature of 340 K, Base Temperature of 341 K. The geometry and ambient air temperature remains the same as in Case I. The total heat loss due to radiation in this case will be 0.084 W. With high emissivity paint (0.98) the radiation loss can be increased to 1.18 W.

3.6 Natural Convection Case: Pentium II Analysis

In order to achieve proper cooling of the processor, a thermal solution i.e. heat sink must make firm contact to the exposed processor die. During all operating environments, the processor case temperature, T_{case} , must be within the specified range of 0 to 100 Deg C. (Intel, 2003). Thermal design power (TDP) for 333 MHz processor is about 11.8 Watts. This TDPmax is a specification of the total power dissipation of the processor while executing a worst-case instruction mix under normal operating conditions at normal voltages. It includes the power dissipated by all of the components within the processor specified by design / characterization.

The thermal solution used for cooling PII processor chip is as shown in figure 3.13. The dimensions are shown in following figure 3.14.

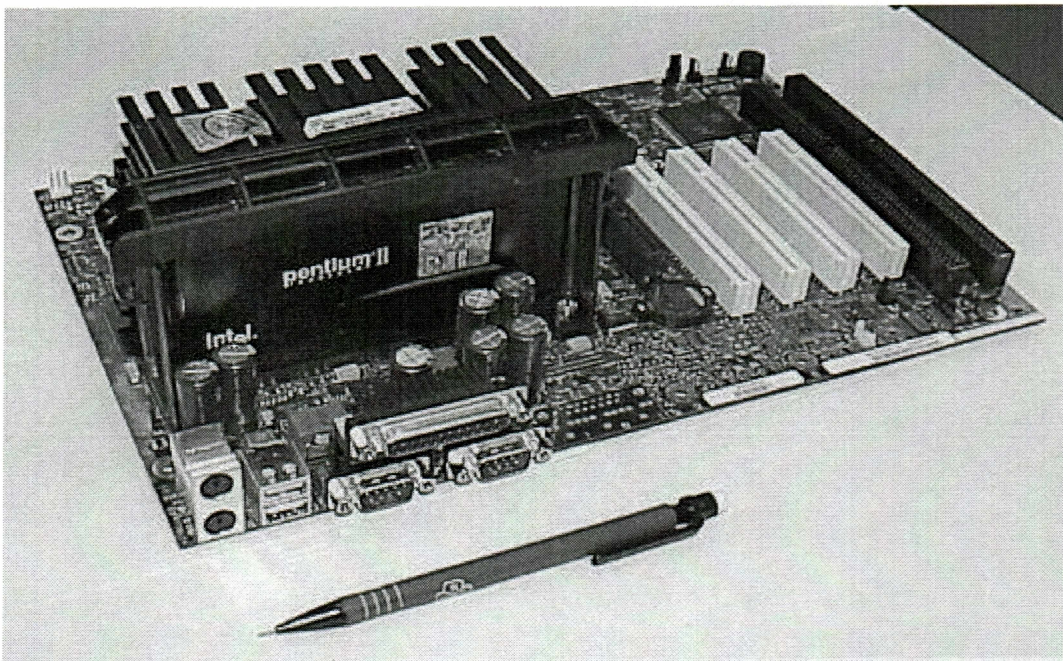


Figure 3.13 Layout of Pentium II processor with heat sink.

In this type of configuration, because of absence of the fan the heat loss is mainly due to natural convection and radiation. The fins are horizontal to the ground. All dimensions of the fins are depicted in Figure 3.14.

In Figure 3.14a, different dimensions from the top are shown and in figure 3.14.b side dimensions are shown.

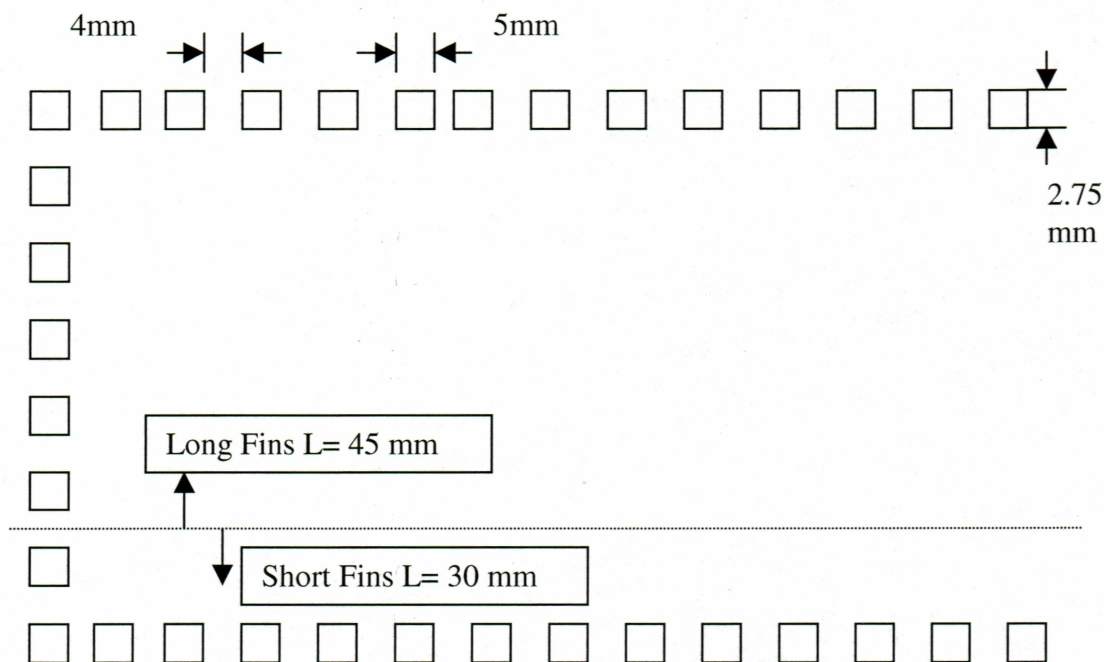


Figure 3.14(a) Schematic of fins with different dimensions.

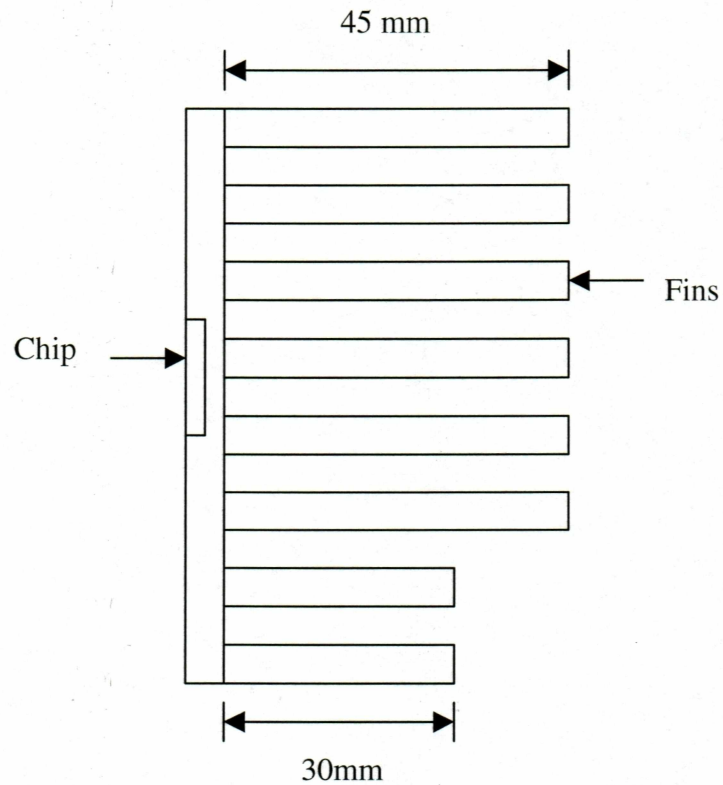


Figure 3.14(b) Side schematic of fins for Pentium II processor.

Case 1: Horizontal plate heated upwards

The correlations used to find Nusselt number is mainly dependant upon Rayleigh number Ra_L . It is given by equation (Suryanarayana, 1995)

$$Ra_L = \frac{g * \beta * (T_s - T_\infty) * L^3}{\alpha * \nu} \quad (3.7)$$

where L is the characteristic length = A_c/P

$A_c = 45 \times 5 = 225 \text{ mm}^2$ and Perimeter (P) = 100mm

Therefore $L = 2.25 \text{ mm}$

Properties of air at 318 K is given by (Incropera, Dewitt 2002)

$$\alpha = 25.164 \times 10^{-6} \text{ m}^2 / \text{s} \quad \nu = 17.7 \times 10^{-6} \text{ m}^2 / \text{s}$$

Substituting these values Rayleigh number comes out to be 26.12, which is very low.

Nusselts number for $1 < Ra_L < 200$ is given by (Suryanarayana, 1995)

$$Nu_L = 0.96 Ra_L^{1/6} = 1.6536 \quad (3.8)$$

and so $h = 20.3 \text{ W/m}^2\text{K}$

Case 2: Horizontal Plate heated downwards

As the correlations are not available for such low Rayleigh number in this case, we will use correlation given by (Suryanarayana, 1995) for $10^5 < Ra_L < 10^{10}$

$$Nu_L = 0.27 Ra_L^{1/4} = 0.61 \quad (3.9)$$

and so $h = 7.49 \text{ W/m}^2\text{K}$

Case 3: For vertical plate:

The natural convection for vertical plate correlations is given by Churchill and presented by (Suryanarayana, 1995)

$$Nu_L = 0.68 + \frac{0.67 Ra_L^{1/4}}{[1 + (0.492 / Pr)^{9/16}]^{4/9}} \quad \text{for } 10^{-1} < Ra_L < 10^9 \quad (3.10)$$

$h = 20.92 \text{ W/m}^2\text{K}$

For natural convection h values for air obtained from Equations (3.8) and (3.10) are high when compared with 5 to 15 $\text{W/m}^2\text{K}$ range given in Table 1.4.1 by Suryanarayana, 1995.

3.6.1 Radiation Analysis in Pentium II Fins

First of all we assumed that the heat sink fins are coated with a material whose emissivity is 0.9. There will be two shape factors, one for sides along columns and other for sides along rows. The shape factor for column wise 156 sides, with spacing of 4 mm between fin and the mid-plane of gap between the fins, is 0.62. Similarly shape factor for row wise 140 sides with the spacing of 7.5mm is 0.73. The other faces of the fins are having shape factor of 1. There are 84 fins having length of 45 mm and 28 fins of length 30 mm. Figure (3.15) shows the variation of heat loss due to radiation with respect to varying surface temperature.

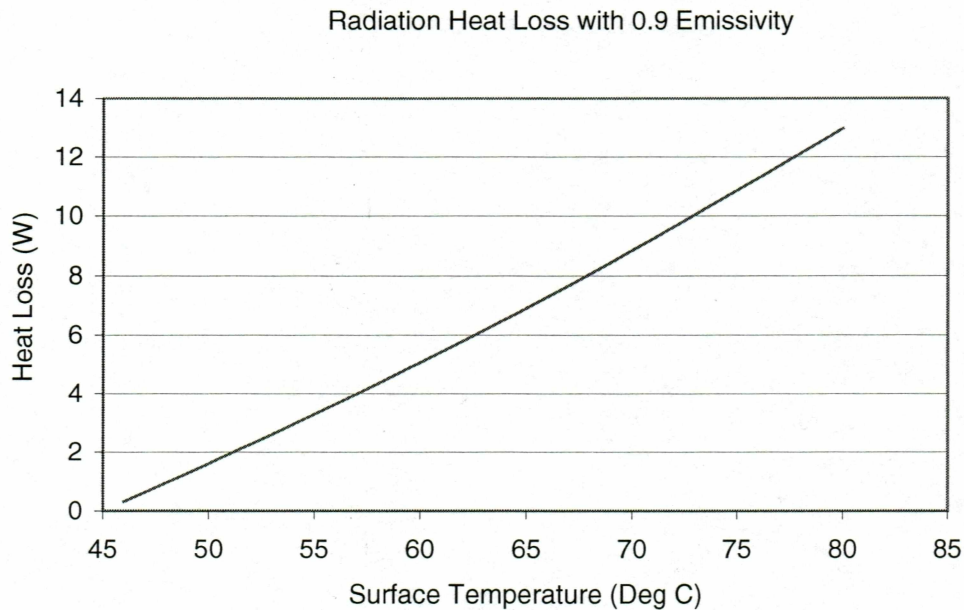


Figure 3.15 Effect of surface temperature on heat loss from the fins.

Now supposing that fins have steady state temperature of 65 Deg C, then heat loss by all fins assuming emissivity of coating 0.9 is 6.91 W. We know from Intel Data sheet that processor has to dissipate 12 W of heat to the environment. So remaining $(12 - 6.91)$ 5.09 W of heat is to be removed by natural convection.

Hence choosing lower limit of heat transfer coefficient of $5 \text{ W/m}^2\text{K}$, find out the surface temperature required to dissipate this 5.09 W . First finding the total surface area available to dissipate heat.

Long Fins: $[(45 \times 5) + (45 \times 2.75)]168 = 58590 \text{ mm}^2$

Short Fins: $[(30 \times 5) + (30 \times 2.75)] 56 = 13020 \text{ mm}^2$.

Total surface area available = 0.07161 m^2

From Newton's law of cooling

$$q = h * A * (T_s - T_f)$$

From above Equation we found the temperature of surface to be 59.2 Deg C , which is less than that of 65 Deg C . At this temperature, natural convection can take all the heat away very efficiently.

3.7 Boundary Layer Thickness

In our analysis, we assumed in Section 3.3.1 that airflow over the fin surface grows unrestrained as on a flat plate boundary layer. In exact analysis, we have to study the merge of the boundary layer between two fins and turning it to fully developed flow.

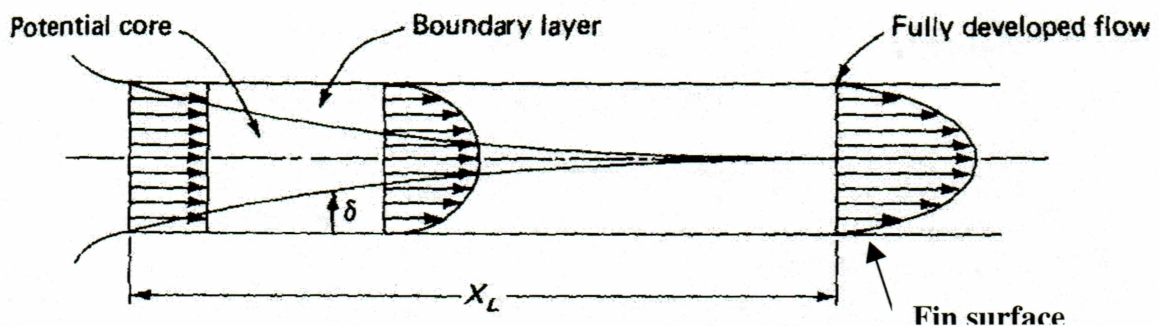


Figure 3.16 Schematic of boundary layer development.

From Figure 3.16 we can easily see that as the flow enters in a channel, the boundary layer thickness starts growing from the leading edge of both the plates. At a distance of X_L both the boundary layer meets each other and after this the flow becomes fully developed. Then we can use correlations available for fully developed flow for the rectangular cross section.

For laminar boundary layers over a flat plate, The velocity boundary layer thickness is given by

$$\frac{\delta}{L} = \frac{5.0}{\sqrt{\text{Re}_L}} \quad (3.11)$$

From equation (3.11), we found out the boundary layer development over flat plate for different velocities and is graphically shown as in figure 3.17.

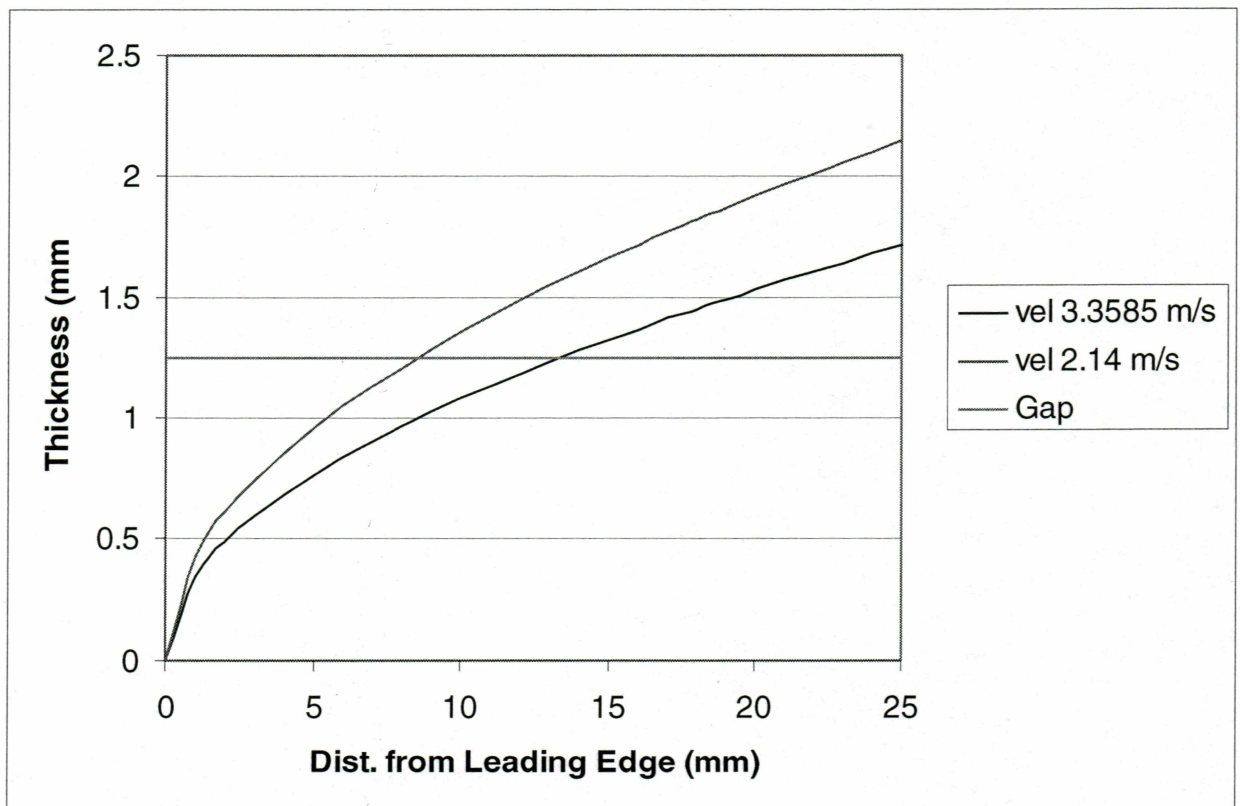


Figure 3.17 Development of boundary layer for different velocities.

From the Figure 3.17 we can conclude that the available gap is 1.25 mm and after that the flow over one surface merged with the flow from surface of other fin. For velocity of 3.3585 m/s the flow get merged at a length of 13.5 mm from leading edge and for velocity of 2.14 m/s, 8.6 mm. Referring to Figure 3.16, after fully developed flow through fin gap we can use the correlations for the flow through rectangular channel. The variation of heat transfer coefficient h is shown in Figure 3.18.

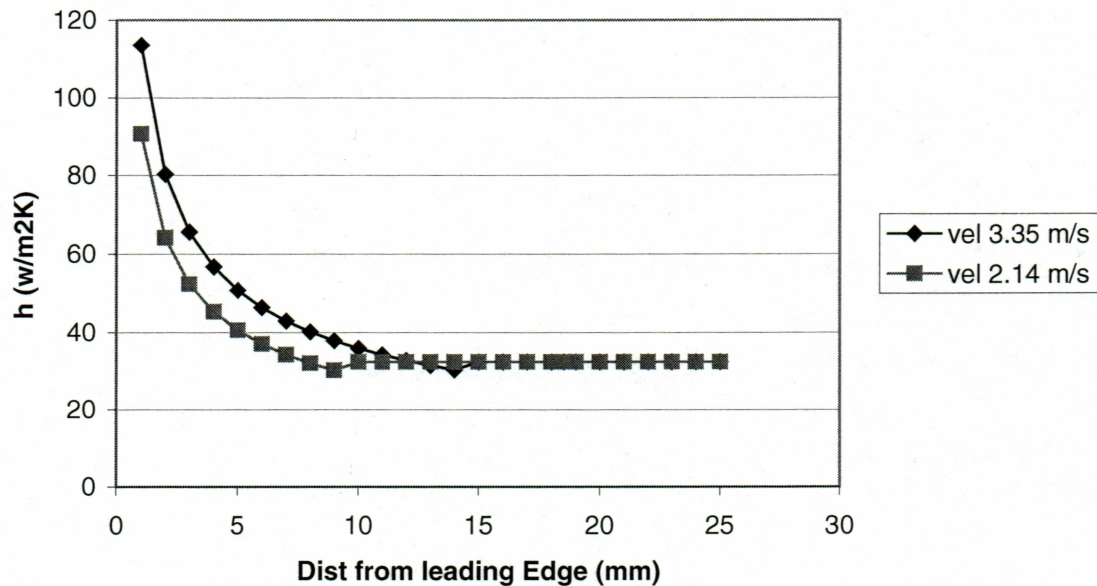
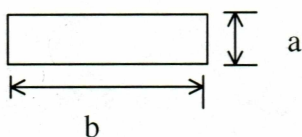


Figure 3.18 Variation of heat transfer coefficient h from leading edge.

3.7.1 Refinement of Heat Loss from Fins

For the fully developed flow flowing through the rectangular cross section as shown below, the Nusselt number is given by Holman, (2001). Nusselt number is given according to the ratio of length (b) to the width (a) of rectangular cross section.



In our case b/a ratio is $25/2.5=10$

From chart (Holman, 2001) for b/a ratio of 10 Nusselts number is 5.604.

Cross Sectional Area $A_c = 62.5 \text{ mm}^2$ and Perimeter $P = 55 \text{ mm}$.

Hydraulic diameter $D_h = 4A_c/P = 4.54 \text{ mm}$

$$h = \text{Nu} \cdot k / D_h = 32.34 \text{ W/m}^2\text{K}$$

Using above heat transfer coefficient we can found out for the velocity of 2.14 m/s the heat loss is 28 W from 10 fins and 32 W for the velocity of 3.35 m/s

3.8 Numerical Analysis

3.8.1 Introduction

Numerical methods provide an easy means of validating and visualizing physical processes besides being economically viable. We used a CFD code Fluent to validate our analytical results in 2D and 3D. A brief summary of the modeling software Gambit and the actual solver Fluent is given below.

GAMBIT:

Gambit is a user-friendly model and mesh generating software. It supports a Graphical User Interface (GUI) that allows the user to draw computational domains with

ease. Gambit comprises eight components that are meant for creating and meshing the computational model.

- (1) A graphics window, in which the user draws the actual model.
- (2) A main menu bar that is meant for general Gambit operations like choosing the solver, saving the model, editing, exporting, *et cetera*.
- (3) Operation toolpad, through which the user creates and meshes the model required.
- (4) Subpads, those assist in the creation and refinement of the model.
- (5) Global control toolpad that allows the user to control the layout and operation of the graphics window.
- (6) Description window, which displays messages to the user describing the various GUI components.
- (7) Transcript window, which displays a log of commands executed and displayed messages.
- (8) Command text box that allows the user to create and mesh a model via the keyboard.

The model thus created is exported into Fluent to be solved. A brief description of Fluent is also given below.

Fluent:

Fluent is a multi-purpose fluid dynamics software, based on the finite volume method that is being used in our numerical calculation. The source code is basically written in C language. One of the very important features of Fluent is its capability to deal with unstructured meshes that are required for complex geometries. In addition, Fluent also provides the user with an easy-to-understand graphics window (the user can also create a graphics window according to his requirements).

The following are the usual steps the user follows while doing a numerical analysis and precisely, we followed most of them.

- (1) Model creation and meshing.
- (2) Selection of solver for 2D or 3D.

- (3) Importing and checking of the grid.
- (4) Selecting the solver formulation and basic equations.
- (5) Specification of material properties and boundary conditions.
- (6) Adjustment of solution parameters and initialization of solution.
- (7) Solution of the problem and post-processing.
- (8) Repeat steps 1 to 7 till desired answers arrive.

3.8.2 Problem Description in a Two Dimensional Domain

We already did the analytical analysis of fluid flow and heat transfer for flow over fins. We are mainly interested in velocity distribution, Nusselt number and heat transfer coefficient of flow. Here we will model two-dimensional plane, which will be the mid-plane of the gap between two fins. We will try to generalize this flow over the total gap between the fins. Here we have investigated our results for 2D and 3D. The problem is of two-dimensional flow with constant viscosity and density. The general continuity equation is

$$\frac{\partial u}{\partial x} + \frac{\partial v}{\partial y} + \frac{\partial w}{\partial z} = 0 \quad (3.12)$$

We have assumed that there is no body force and no pressure gradient along the flow as the flow is over the surfaces of plane fins. This is a steady state problem so terms with time dependence goes to zero. Assuming flat plate type of flow over fin surfaces the Navier-Stokes equation reduces to

$$u \frac{\partial u}{\partial x} + v \frac{\partial u}{\partial y} + w \frac{\partial u}{\partial z} = -\frac{1}{\rho} \frac{\partial p}{\partial x} + \nu \left(\frac{\partial^2 u}{\partial x^2} + \frac{\partial^2 u}{\partial y^2} + \frac{\partial^2 u}{\partial z^2} \right) \text{ X momentum equation (3.13)}$$

$$u \frac{\partial v}{\partial x} + v \frac{\partial v}{\partial y} + w \frac{\partial v}{\partial z} = -\frac{1}{\rho} \frac{\partial p}{\partial y} + \nu \left(\frac{\partial^2 v}{\partial x^2} + \frac{\partial^2 v}{\partial y^2} + \frac{\partial^2 v}{\partial z^2} \right) \text{ Y momentum equation (3.14)}$$

$$u \frac{\partial w}{\partial x} + v \frac{\partial w}{\partial y} + w \frac{\partial w}{\partial z} = -\frac{1}{\rho} \frac{\partial p}{\partial z} + \nu \left(\frac{\partial^2 w}{\partial x^2} + \frac{\partial^2 w}{\partial y^2} + \frac{\partial^2 w}{\partial z^2} \right) \text{ Z momentum equation (3.15)}$$

$$u \frac{\partial T}{\partial x} + v \frac{\partial T}{\partial y} + w \frac{\partial T}{\partial z} = \frac{k}{\rho C_p} \left(\frac{\partial^2 T}{\partial x^2} + \frac{\partial^2 T}{\partial y^2} + \frac{\partial^2 T}{\partial z^2} \right) + \frac{\mu}{\rho C_p} \left[2 \left(\frac{\partial u}{\partial x} \right)^2 + 2 \left(\frac{\partial v}{\partial y} \right)^2 + 2 \left(\frac{\partial w}{\partial z} \right)^2 + \left(\frac{\partial v}{\partial x} + \frac{\partial u}{\partial y} \right)^2 + \left(\frac{\partial w}{\partial y} + \frac{\partial v}{\partial z} \right)^2 + \left(\frac{\partial u}{\partial z} + \frac{\partial w}{\partial x} \right)^2 \right]$$

Energy equation (3.16)

3.8.3 Computational Domain

First of all the domain is created in Gambit Version 2.0.4. Domain here will be 2 dimensional i.e. x and y only. The whole domain is of 25 X 50 units. Gambit is dimensionless grid generation software. This is nothing but the dimensions of mid-plane of flow regime. Gambit has the capability to provide the model inputs to many solvers e.g. Ansys, Fluent etc. Since we are importing the model to Fluent, in Gambit we used the solver as Fluent 6.0

In operation tool we choose geometry then choose face. In face we want to create a rectangle with dimensions of 25 X 50 mm. We choose XY Cartesian System with W= 50 and H=25.

Operation → Geometry → Face → Rectangle

The next step is meshing of face.

3.8.4 Mesh Generation

As there will be much more changes in velocity and heat transfer at the bottom edge of domain, we need finer mesh near the bottom edge. So we will first mesh the vertical edges 1&3. We will grade with successive ratio of 1.05263 and with interval size spacing of 0.5. For horizontal edges 2&4 we will apply grading with successive ration of 1 and interval size spacing of 0.5. After meshing edges according to expected results, we have to mesh the face with these settings. We will use quadrilateral elements with map type. The Quad-map meshing scheme is applicable primarily to faces that are bounded by four or more edges. Map is mainly applied such that mesh represents logical cube (3D) or

rectangle (2D). While creating mapped mesh we have to specify edge mesh intervals such that the numbers of mesh intervals on the opposite sides of the logical rectangle are equal.

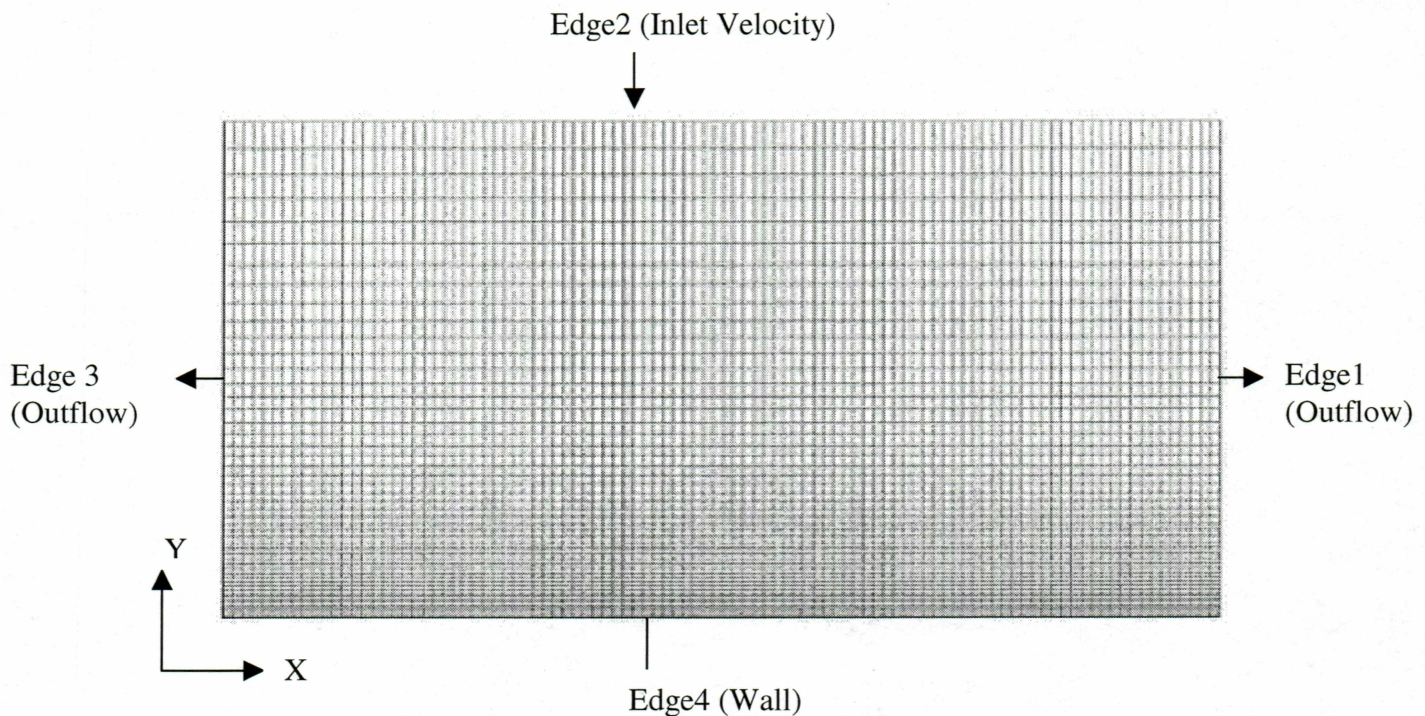


Figure 3.19 Details of grid generation.

In Fluent 6 solver we can define different types such as inflow, wall, outflow etc. In our model we defined following boundary conditions. Edge 2 will be Velocity_inlet, Edge 4 Wall and Edges 1 & 3 will be outflow. So the air in our case will be coming from edge 2 hits the wall edge 4 gets split into symmetric flow and passes out through edges 1&3. In this grid we used 5000 quadrilateral cells with 5151 node elements. Then we can save this meshing and export *.msh file to Fluent.

In Fluent we will read this case and check for grid. In Grid check we have to check for volume and area to ensure it is not negative. In Grid menu we have to set scale first. Our domain is 25 mm x 50mm. Change the length units to millimeters.

Next step is defining models, materials, operating conditions, boundary conditions and units. We can check units of velocity to m/s. We chose segregated, implicit, 2D, steady state with absolute velocity formulation. Using segregated approach the governing equations are solved sequentially. Because governing equations are non linear, several iterations of the solution loop must be performed before a converged solution is obtained. In segregated solution the discrete, non-linear governing equations are linearized to produce a system of equation for the dependant variables in every computational cell. The resultant linear system is then solved to yield an updated flow-field solution. We choose implicit because for a given variable, the unknown value in each cell is computed using a relation that includes both existing and unknown values from neighboring cells. Therefore each unknown will appear in more than one equation in the system, and these equations must be solved simultaneously to give the unknown quantities.

Absolute velocity formulation is preferred in applications where the flow in most of the domain is not rotating. From calculations we know Reynolds number is very small, so we can choose Laminar as viscous model. As we are considering heat transfer also we will enable energy equation also. In material we will use air as our fluid flowing through fins. The properties of air used here are as follows

Density (constant) 1.225 kg/m³, Specific heat of 1006.4 J/kg-K, Thermal conductivity of 0.0242 w/mK and viscosity of 1.78 E -05. The operating pressure is atmospheric pressure and we will not consider the gravity effect. In boundary conditions, we set the inflow velocity of 2.14 and 3.3585 m/s constant normal to edge 2 at temperature of 318K. Outflow is defined by flow rate weighting 1. For wall boundary condition we defined constant temperature of 353 K. The name of material for wall is Aluminum. The convergence criteria for running the case are used by default. The criteria for continuity, x velocity and y velocity is 0.001 and for energy it is 1e-06. We will initialize our run from inflow. We will create iso surface to check the velocity at some distance from the wall. We created iso surfaces at y=1,3,5,7,10,15,20 and 24 mm in y direction. After running through iterations the solution will get converged which gives us results.

3.8.5 Post processing of Results

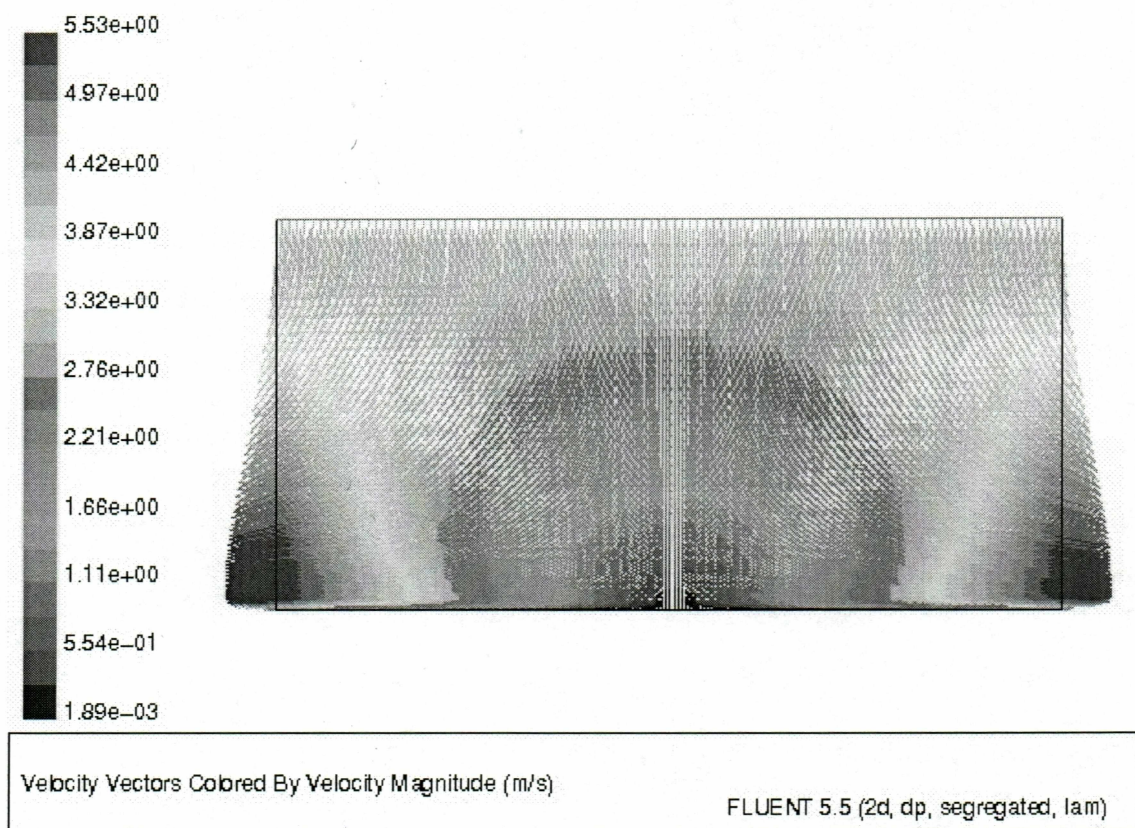


Figure 3.20 Velocity Distribution over a fin with Inlet velocity of 3.3585 m/s

Figure 3.20 shows the details of velocity variation for inlet velocity of 3.35 m/s. This velocity ranges from 1.89 mm/s to 5.52 m/s. From figure 3.18 we can easily analyze that as the air approaches to the wall the velocity of air decreases gradually and near the wall it is almost 0 m/s. This is the stagnation point for air i.e. velocity is almost zero. Pressure increases at stagnation point. Then this airflow gets split up in to two symmetrical flows of equal volume flow rate. Then this air gushes out with a high speed at the outlet. According to this variation of velocity the Nusselt number and heat transfer coefficient is also get varied. To find the exact velocity profile at different sections, we

already created isosurface at $y = 1, 3, 5, 7, 10, 15, 20$ and 24 mm. We recorded the velocity and plotted the graph along the length. This is shown as in figure 3.21

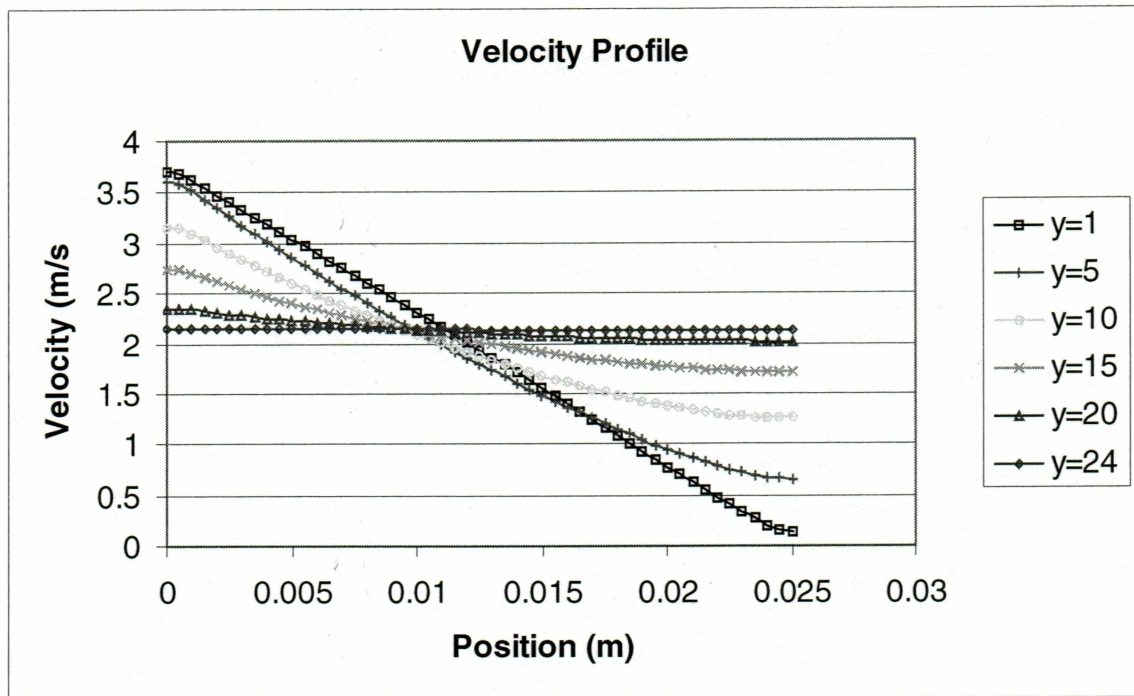


Figure 3.21 Velocity distribution at various cross sections of y with inlet velocity of 2.14 m/s

In figure 3.21 we can see that at $y=1$ mm, the slope of velocity line decreases more rapidly. This means at the outlet, at $y=1$ mm the velocity of air is very high and at the midsection i.e. at $y=25$ mm the velocity is nearly zero.

The same graph is plotted for inlet velocity of 3.3585 m/s. This is shown in figure 3.22.

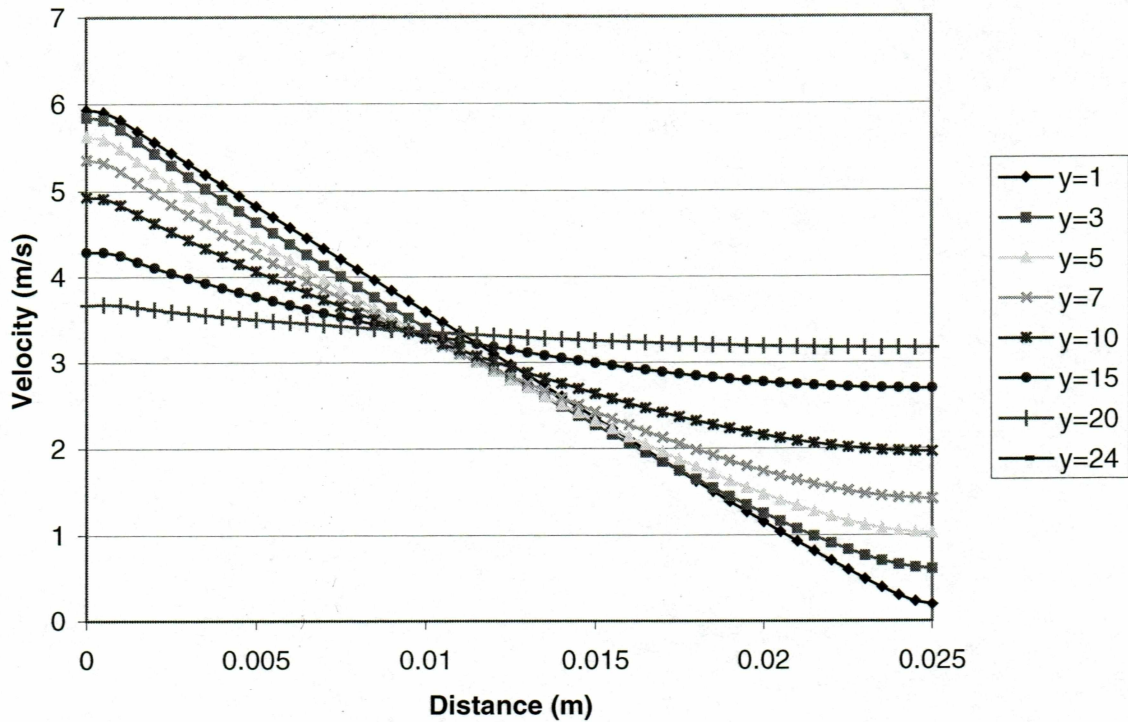


Figure 3.22 Velocity distribution at various cross sections of y with inlet velocity of 3.3585 m/s

For the next analysis to find out heat transfer coefficient, we considered that this velocity prevails till the midplane of next stage. For example we considered two velocity profile i.e. at $y = 1\text{ mm}$ and at $y = 3\text{ mm}$. The velocity profile at $y = 1\text{ mm}$ will prevail till $y = 2\text{ mm}$ and after that velocity profile of $y = 3$ will dominate. This is a very good approximation technique to find out overall heat transfer coefficient and finally heat loss by each fin. This variation is shown in Table 3.5 and Table 3.6 for two different velocities.

Table 3.5 Heat Loss from one fin for 2.14 m/s velocity at 45 deg C

| Position Y mm | Heat Transfer Coefficient h w/mK | Heat loss w |
|---------------|-------------------------------------|----------------|
| 2 | 15.544 | 0.135 |
| 4 | 15.65 | 0.136 |
| 6 | 15.87 | 0.137 |
| 8.5 | 16.14 | 0.168 |
| 12.5 | 16.54 | 0.285 |
| 17.5 | 17.08 | 0.326 |
| 22 | 17.32 | 0.301 |
| 24.13 | 17.4 | 0.159 |
| | Total Heat Loss | 1.62 |

From the table we can conclude that heat loss from 10 fins is about 16.2 watts

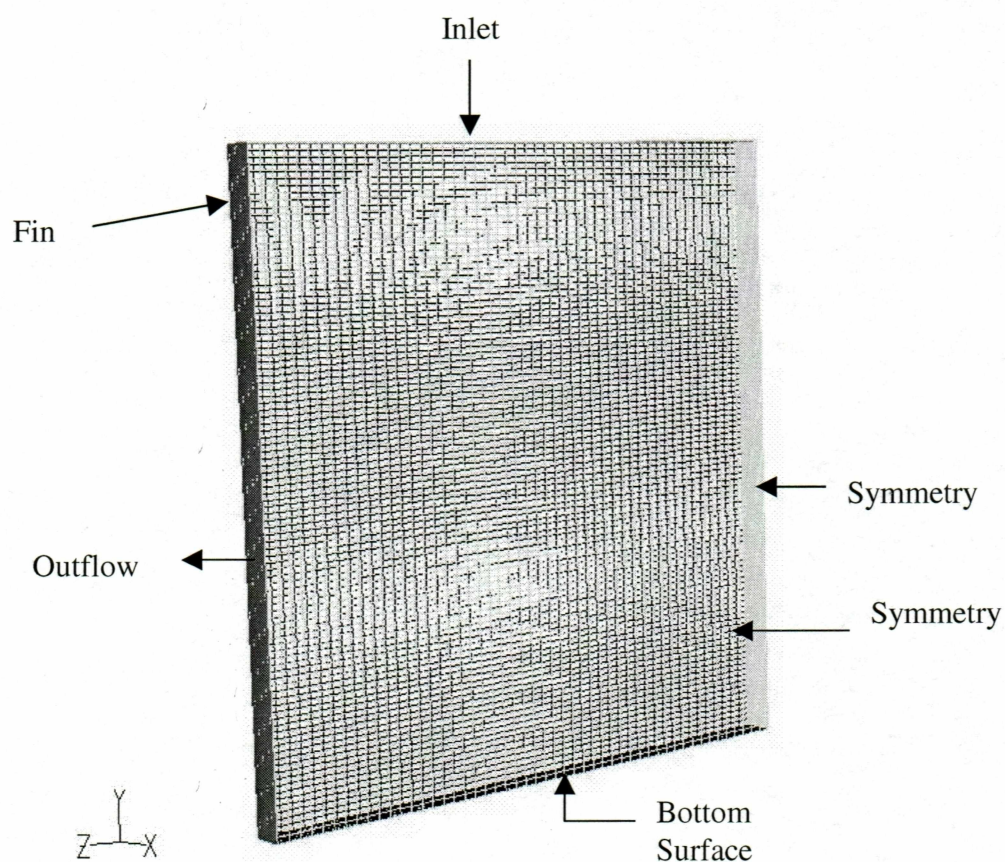
Table 3.6 Heat Loss from one fin for 3.3585 m/s velocity at 45 Deg C

| Position Y mm | Heat Transfer Coefficient h w/mK | Heat Loss w |
|---------------|-------------------------------------|----------------|
| 2 | 19.43 | 0.397 |
| 4 | 19.54 | 0.400 |
| 6 | 19.84 | 0.406 |
| 8.5 | 20.195 | 0.495 |
| 12.5 | 20.725 | 0.763 |
| 17.5 | 21.405 | 0.962 |
| 22 | 21.704 | 0.887 |
| 24.13 | 21.756 | 0.468 |
| | Total Heat Loss | 4.778 |

From the table we can conclude that heat loss from 10 fins is about 47.78 watts

3.8.6 Three Dimensional Analysis

After getting satisfactory results in two-dimensional analysis, we built a realistic three-dimensional model to accurately predict the real flow and heat transfer characteristics. The domain used here is half of the gap between the fins, as they are symmetric. The pattern for velocity profile in two-dimensional flow over the fin about a vertical axis is symmetric. Therefore, we selected half the fin length as our domain length. Three-dimensional domain is shown below in Figure 3.23.



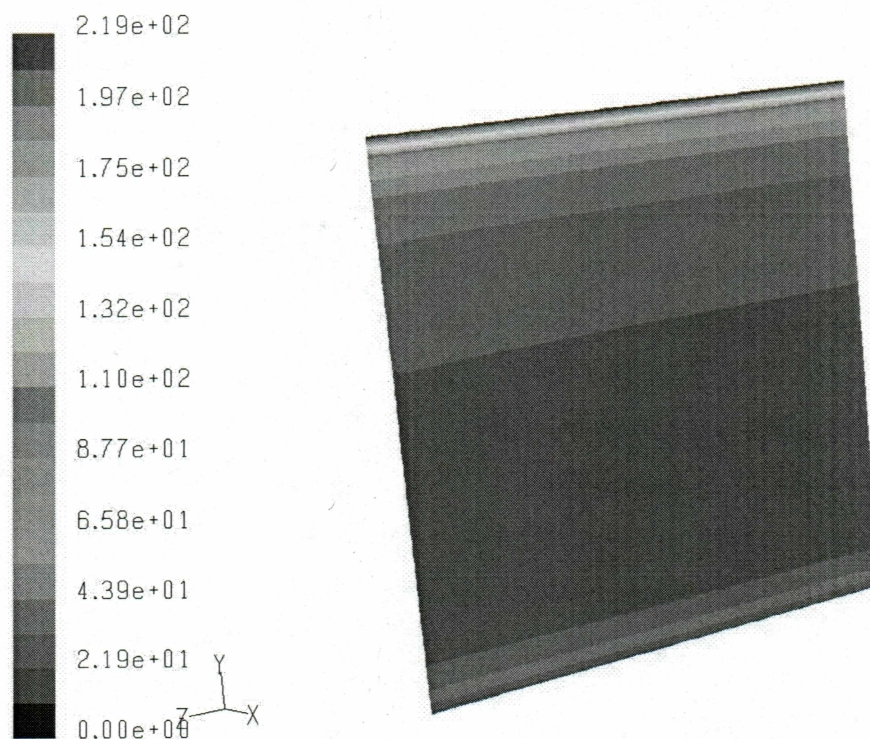
Grid

 Jul 16, 2003
 FLUENT 6.0 (3d, dp, segregated, lam)

Figure 3.23 Computational domain for 3D analysis.

The dimensions of the domain are 25 X 25 X 1.25 mm in X,Y,Z directions respectively. Z dimension is the length of the fin. Y dimension is the height of the fin. X dimension is the length between the fin and the midplane of the gap between the adjacent fins. Boundary conditions for this analysis are: YZ plane at $X = 0$ is the fin with constant wall temperature of 79 Deg C. This 79 Deg C is the average temperature from the base to the tip of the fin. Another YZ plane at $X = 1.25$ mm acts as a plane of symmetry for both velocity and temperature, where normal velocity vector and heat flux are considered to be zero. XY plane at $Z = 0$ acts as symmetry of flow and other XY plane at $Z = 25$ mm acts as outflow boundary with flow rate weighting factor of 1. If the flow is divided equally among all the outflow boundaries then weighing factor is considered to be 1. XZ plane at $Y = 25$ mm is inlet, where air enters in perpendicular direction to this plane with velocities of 3.35 m/s and 2.14 m/s for two different cases. Air entering in this system is assumed to be at ambient condition i.e. at 45 Deg C. Another XZ plane at $Y = 0$ is bottom wall with constant temperature of 80 Deg C. Mesh is automatically generated in Gambit. There are 65000 hexahedral cells with 72114 binary nodes. The cells are of same size. All other properties are same as two-dimensional case discussed in Section 3.8.4. The results of the three-dimensional computations are shown below.

3.8.7 Post processing of 3D Results



Contours of Surface Heat Transfer Coef. (w/m²-k)

Jul 13, 2003
FLUENT 6.0 (3d, dp, segregated, lam)

Figure 3.24 Contours of heat transfer coefficient over the fin surface for a velocity of 3.35 m/s

From the Figure 3.24 we can analyze that as the air flows over the fin, the boundary layer will start growing over the fin. As the boundary layer theory dictates, the heat transfer coefficient value will be highest at the leading edge and we obtain 219 W/m²K in our simulations. From there it decreases towards the bottom as the boundary layer approaches the fully developed flow condition. In the region towards the bottom of the channel, we observed that there is existence of a reverse flow region. Because of this reverse flow the boundary layer get separated. Also in this reverse flow region velocities are of lower magnitude. Hence we observe lower value of heat transfer coefficient, around 22 W/m²K, near the bottom surface. The total heat loss from one fin surface alone

is about 2.3 W and from the bottom is around 0.038 W. Hence the total heat loss from all 10 fins (20 faces and 9 bases) is found to be 46.6 W.

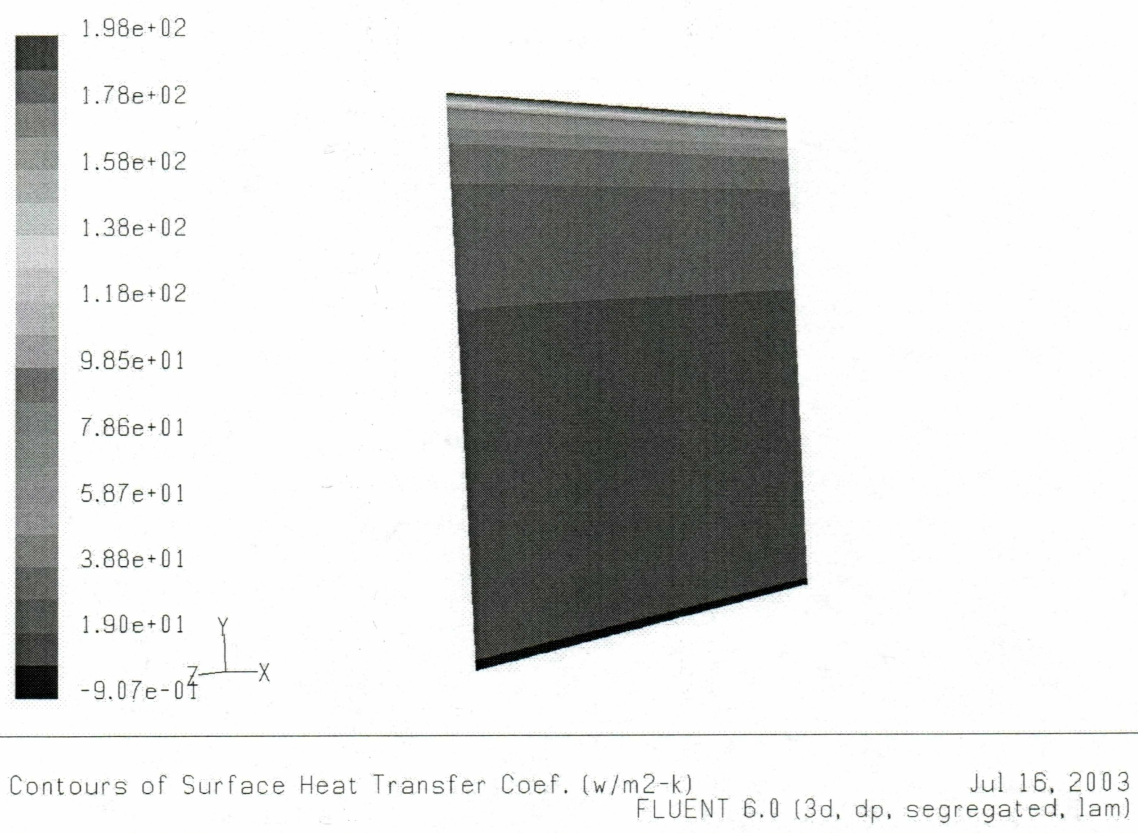


Figure 3.25 Contours of heat transfer coefficient over the fins surface for a velocity of 2.14 m/s.

From Figure 3.25, we observed exactly similar results as discussed in the previous paragraph. The h value over the fin ranges from 192 W/m²k to a very small value. This is due to low inlet velocity and a broader recirculating zone. The flow pattern is same as for 3.35 m/s. The total heat loss from one fin surface alone is about 1.86 W and from the bottom is around 0.08 W. Hence the total heat loss from all 10 fins (20 faces and 9 bases) is found to be 38.84 W.

CHAPTER FOUR

APPLICATION TO MICROSCALE CHIPS

As seen in earlier chapters we have designed a model of the heat sink, which will dissipate 24 Watts efficiently. Next we have to design a heat sink for Nano-Blocks. In a demonstration for Fluidic Self Assembly at UAF, by Alien Technology (Personal communications, 2002) we were given the dimensions of Nano-Blocks, which are $600 \times 600 \mu\text{m}$ dissipating approximately 5 mW of thermal power. Therefore, by scaling rules, we have reduced dimensions of the heat sink based on a small amount dissipated power. Next, we should analyze whether this scaled heat sink design is thermally efficient or not. We have adopted similar kinds of specifications that were done in macroscale analysis in Chapter 3.

4.1 Specifications

- 1) Thermal Design Power (TDP) is 3.9 mW based upon our scaling law and as a factor of safety we increase it to 5 mW.
- 2) Maximum junction temperature T_j , as used earlier, is limited to 80 Deg C.
- 3) Dimensions of chip are $600 \mu\text{m} \times 600 \mu\text{m} \times 60 \mu\text{m}$. It is made up of silicon.

The heat sink is made up of pure aluminum. The properties of the silicon and aluminum are same as noted in Chapter 3.

4.1.1 Scaled Dimensions

We have scaled down all dimensions of heat sink, which was presented in chapter 3, based upon the microchip dimensions. The dimensions of the heat sink after scaling is given in Figure 4.1.

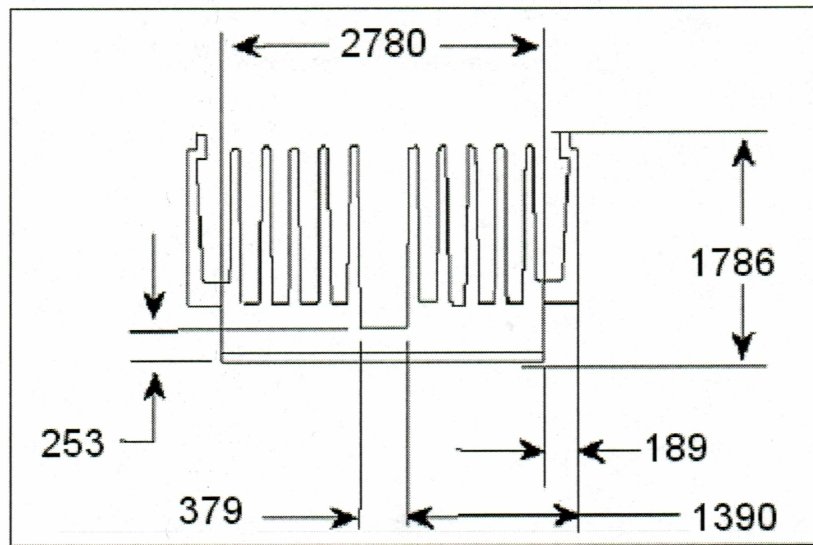


Figure 4.1 Scaled heat sink geometry with dimensions in micrometers.

4.2 Need for the Heat Sink

First of all we must check whether the exposed top surface of the microchip is capable of dissipating 5 mW of heat to the surroundings by natural convection and radiation. If so then we don't need a heat sink. The available surface area for the chip to dissipate heat is $0.36 \times 10^{-6} \text{ m}^2$. Let us assume an approximate emissivity of 0.9 and a view factor of 1 as an upper limit. The surface temperature of the chip is held constant at the junction temperature of 80 Deg C and a fluid temperature of 45 Deg C is assumed. From Equation (2.22) the heat loss by radiation is 0.097 mW.

Taking a conservative value of heat transfer coefficient h for natural convection as $5 \text{ W/m}^2\text{K}$, the heat loss by free convection is given by Equation (2.10) and it is 0.063 mW. Therefore total heat loss by convection and radiation is 0.16 mW. However, 5 mW must be dissipated. From this analysis we can conclude that we need a heat sink for surface area enhancement.

4.3 Conduction Analysis for the Miniaturized Chip and Sink

4.3.1 Temperature Distribution in the Chip from Heat Generation Theory

Another limitation to be observed is that the case temperature of chip should not exceed 69 Deg C to be in good operation. The available boundary condition for the chip surface facing the printed circuit board should be at 69 Deg C. The second boundary condition is a known heat flux from continuous generation of heat of 5 mW and that flows through the other face of chip to the heat sink.

A schematic diagram of chip placement is shown in Figure 3.2.

The Fourier equation with heat generation is given by Equation (2.2)

$$q''' = Q/V = 0.23 * 10^9 \text{ W} / \text{m}^3 \quad (4.1)$$

Integrating Equation (2.2) twice and applying the two boundary conditions of known heat flux and case temperature of 69 Deg C at the bottom, we obtain the final equation for temperature distribution in the chip, where x is measured from the center.

$$T = \frac{-q'' x^2}{2k} - 46.916 * x + 68.9992 \quad (4.2)$$

From Equation (4.2) the change in temperature dT is calculated in the chip and is shown in Figure 4.2. Here the unit of dT is in milliKelvin.

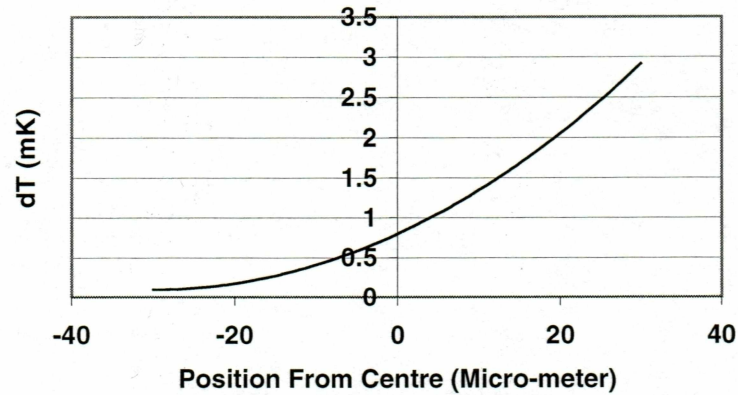


Figure 4.2 Change in temperature (milliKelvin) profile in the processor chip.

From the plot in Figure 4.2 it is seen that temperature of the top surface (+ side) of the chip is about 68.997 DegC. From this figure we observe that the temperature difference between the top and bottom surface of the chip is 3 milliKelvin. Temperature dT changes from 0 to 3 milliKelvin from the bottom to the top of the chip.

4.3.2 Interface Resistance with a Bond Material

We adopted Aluminum Nitride as the bonding material having $K = 230 \text{ W/mK}$ (Bar-Cohen & Kraus, 1990) and an average bond thickness of $6.84 \mu\text{m}$ (Lee, S., 1995). From equation (2.8) we found the temperature drop across the bond is 0.413 mK. This is desirable, since efficient heat transfer demands least resistance to heat flow from the chip to the heat sink.

4.3.3 Spreading Resistance to the Substrate

When the chip as a heat source sits on a thick substrate or heat spreader, there is additional thermal resistance due to lateral heat flow as illustrated in Figure 2.2 in Chapter 2 and given by Equation (2.9).

In this microscale case $\varepsilon_1 = 0.044$, $a = 600 \mu\text{m}$ and aluminum block is taken as the heat spreader. Hence spreading resistance R_{sp} is $0.65 ^\circ\text{C/W}$.

Another approach for calculating spreading resistance is also available (Jamina, 2003). According to this approach, as shown in Figure 4.3, when heat flows from die

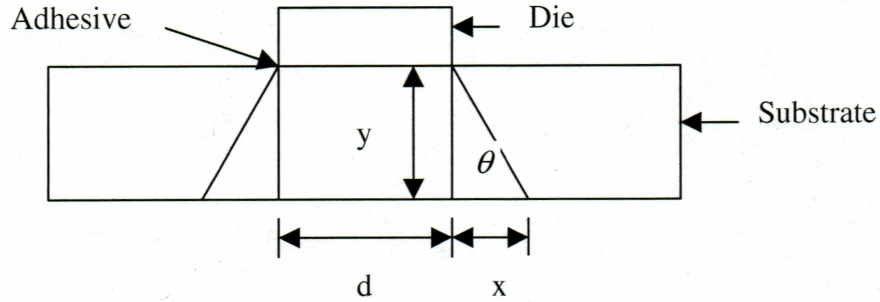


Figure 4.3 Schematic of heat spreading cone.

surface to the substrate, it spreads in a conical fashion. It progressively covers a larger area. The cone angle θ depends on the thermal conductivity of the substrate material. Jamina (2003) recommends using an average area of the top and bottom surfaces. To calculate this area, the cone angle must be known. The following correlation is available to find the cone angle.

$$\theta = 90 \tanh\{0.355(\pi K / 180)^{0.6}\} \quad (4.3)$$

where K is the thermal conductivity of the substrate material. In our case K for Aluminum is 240 W/mC . From Equation (4.3), we calculated $\theta = 61.65^\circ$. For a one-dimensional problem depicted in Figure 4.3, heat spreading is assumed in the x - y plane and the depth L is perpendicular to the paper.

$$\text{Then } x = y \tan(\theta) \quad (4.4)$$

$$\text{and average area} = (d + x)L \quad (4.5)$$

for the microscale case $y = 67 \text{ micrometer}$. From equation (4.4) $x = 124.17 \text{ micrometer}$ and so average area is 0.048 mm^2 . Resistance across the aluminum is given by

$$R = (L/KA) \quad (4.6)$$

From equation (4.6) resistance is $5.81 ^\circ\text{C/W}$.

Thus the temperature difference across the aluminum spreader, which forms the base of the heat sink, will be 0.03 Deg C. This is negligibly small. Therefore, we are justified in our analysis by neglecting the spreading resistance.

4.3.4 Steady State Heat Conduction in the Sink Base

As shown in Figures 3.1 & 3.2, the processor microchip that generates heat is attached to the aluminum heat sink by a bonding compound. Heat is conducted through this bonding layer into the base of the aluminum heat sink and from there to the fins. The thermal analysis is based on one-dimensional steady state heat conduction, through this 67 μ m thick aluminum base.

The input parameters for analysis is a heat flow of 5 mW from side at $x=0$ at the bottom in Figure 3.2. To determine the upper limit of heat flow, we first adopt a maximum junction temperature of 80 Deg C. The base of the heat sink is treated as a slab of 67 μ m thick. The dimension of heat sink base is 2.8 mm X 2.9 mm.

According to Fourier law of heat conduction

$$Q = k A_x \frac{T_s - T}{L} \quad (4.7)$$

Where Q is 5 mW, which is conducted into the heat sink and is dissipated to the surrounding air from the sink. From Equation (4.7), the temperature at a distance $x=67$ μ m i.e. at the other face of the base slab is 79.99942 Deg C.

4.4 Transient Heat Conduction

As mentioned in Section 3.2.5, transient heat conduction analysis is important to check the steady state temperature and the time to reach that temperature. The final form of equation having dependency of time is given by

$$T(t) = T_o + \frac{q_G}{K_e} (1 - e^{-(K_e / MC_p)t}) \quad (4.8)$$

K_e is the conductance to the environment that consists of conduction as well as convection. It is calculated to be 0.0044 W/ Deg C.

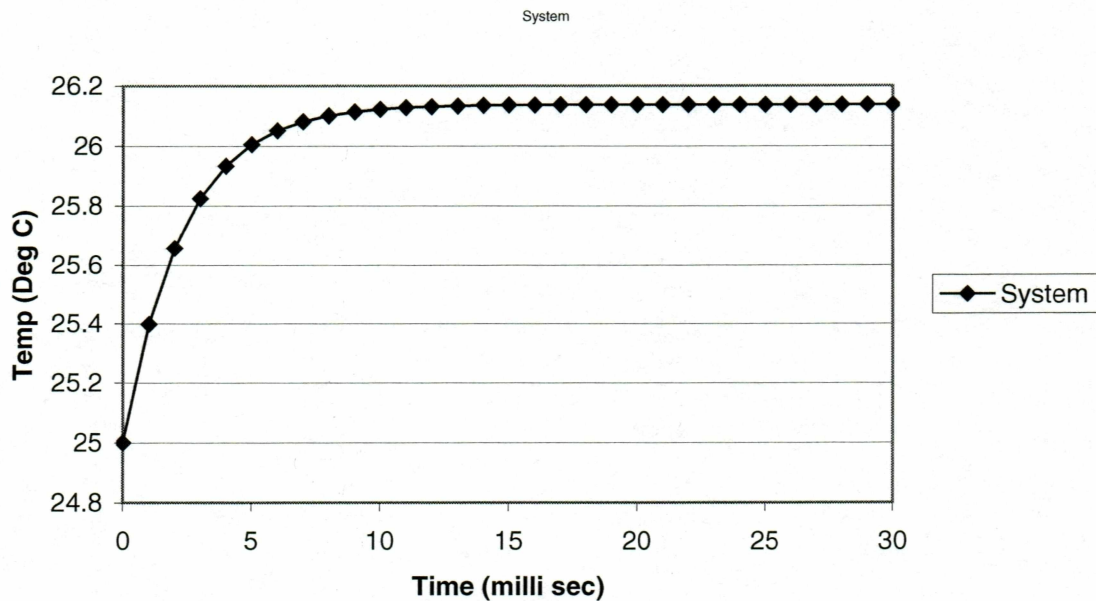


Figure 4.4 Temperature rise in total heat sink until steady state is achieved.

From Figure 4.4 it is observed that for the heat sink system with aluminum, it takes about 18 milliseconds to reach the steady state condition. The steady state temperature attained by the sink is about 26.13 Deg C. Since the steady state temperature is below the required limit of the case temperature of 69 Deg C and having attained the steady state reasonably fast, the heat sink design appears to be a successful one. The chip

mass is less than 1% of the total mass. Therefore, just using the properties of aluminum in calculation is accurate enough.

4.5 Steady State Gas Flow Model

The thickness and spacing between the fins for the heat sink are in micro scale dimension. Therefore the flow of cooling air would be equivalent to flow of fluid through micro-channels. The gas flow in the micro-channel can be in a viscous state, molecular state or in a transition state. The benchmark between laminar, intermediate and molecular flow is given by a dimensionless number called Knudsen Number. It is the ratio of characteristic length of geometry over a mean free path of gas molecule.

$$Kn = \delta / \ell \quad (4.9)$$

Where, ℓ is the mean free path of gas molecules and δ is the characteristics length. The mean free path is very small at atmospheric pressure and so the flow of gas molecules is governed by viscosity. In this viscous range the flow can be laminar or turbulent. Reynold's number defines the distinction between laminar and turbulent flow. If $Re > 2100$ in a channel, then the flow is entirely turbulent. And if $Re < 1100$ (Carlen and Mastrangelo, 2002) the flow is fully laminar. When at low pressure, the mean free path of gas molecules is similar as the characteristic length of micro-channel; flow is governed by viscosity as well as molecular phenomenon. This is called transition state. At extremely low pressure, when mean free path is much larger than channel dimensions, flow is in molecular regime. (Carlen and Mastrangelo, 2002)

Knudsen number range is given as follows:

$$Kn > 110 \quad \text{Laminar Flow regime}$$

$$1 < Kn < 110 \quad \text{Transition Flow regime}$$

$$Kn < 1 \quad \text{Molecular flow regime}$$

The flow regime is tabulated as shown in Table 4.1

Table 4.1 Criteria for different Fluid Regime

| State of Gas | Flow Regime | Condition |
|--------------|--------------|-----------------------|
| Viscous | Turbulent | $Re > 2100$ |
| | Laminar | $Re < 1100; Kn > 110$ |
| Transition | Intermediate | $1 < Kn < 110$ |
| Rarified | Molecular | $Kn < 1$ |

If the boundary layer on fin surfaces do not merge in the microchannel then the Reynolds number distinguishing laminar to turbulent flow is based on flat plate theory, $Re > 5 \times 10^5$.

4.5.1 Mean Free Path Calculation for the Air Molecules

In order to ascertain whether the flow in the channel of the heat sink we have designed is in viscous, transition or rarified range, we must calculate the mean free path. There are different approaches to find the mean free path length of air molecules.

Approach 1:

This is based on the kinetic theory of gas molecules. According to Maxwell theory, the macroscopic concept of viscosity is related to statistical average of momentum exchange occurring between molecules of the fluid. The accepted approximation for nonpolar gases is (White, 1991)

$$\mu \approx 0.67 \rho l a \quad (4.10)$$

According to Chapman and Cowling, viscosity varies slightly with temperature because of collision integral Ω_v , which is computed from an approximate intermolecular force potential between the given molecules of effective collision diameter σ . So the kinetic theory formula for dilute- gas viscosity is (White, 1991)

$$\mu = \frac{2.68E - 6\sqrt{MT}}{\sigma^2 \Omega_v} \quad (4.11)$$

Where σ = collision diameter, Angstrom

M = molecular weight of gas

μ = Viscosity, kg/(m.s)

T = Absolute temperature, K

Ω_v is given by

$$\Omega_v = 1.147 \left(\frac{T}{T_\epsilon} \right)^{-0.145} + \left(\frac{T}{T_\epsilon} + 0.5 \right)^{-2.0} \quad (4.12)$$

For air $\sigma = 3.711A^\circ$ and $T_\epsilon = 78.6$ K

Speed of sound, a (m/s) is given by (White, 1991)

$$a = \sqrt{\gamma RT} \quad \gamma = \frac{c_p}{c_v} = 1.4 \quad (4.13)$$

R= Gas constant, T= Temperature, K

$$R_{air} = \frac{R_{universal}}{M_{air}} = \frac{8313}{28.97} = 287 J / (kg.K)$$

We consider here two air temperature cases $T = 25^\circ C$ corresponding to the starting of cooling when the ambient air has not been heated and $T = 45^\circ C$ the upper limit recommended by computer industry presumably representing long runs of computers when the surrounding air is heated completely.

Case 1: Air temperature of 25 Deg C

From Equation (4.12) $\Omega_v = 0.998$, From Equation (4.11) $\mu = 1.8085E-5$ Kg/(m.s),

$a = 346.03$ m/s. Density of air at 298 K is 1.1774 kg/m³ (White, 1991). So the mean free path of air molecules from Equation (4.10) is $\ell = 6.6253$ E-8 meters.

Case 2 : Air temperature of 45 Deg C

$\Omega_v = 0.985$, $\mu = 1.8962$ E-5 Kg/(m.s), $a = 346.03$ m/s.

Density of air at 318 K is 1.109816 kg/m^3 (White, 1991). So the mean free path of air molecules from Equation (4.10) is $\ell = 7.134 \text{ E-8 meters}$.

Approach 2:

A simple approximate relation for the mean free path of air molecules is given by (Holman, 1990)

$$\ell = 2.27E-5 * \frac{T}{p} \quad (4.14)$$

Where T is temperature in K and p is pressure in Pascals. We will calculate mean free path at atmospheric pressure, 101350 Pascals.

Case 1: Air temperature of 25 Deg C

$$\begin{aligned} \ell &= 2.27E-5 * \frac{298}{101350} \\ &= 6.675 \text{ E-8 meters} \end{aligned}$$

Case 2 : Air temperature of 45 Deg C

$$\begin{aligned} \ell &= 2.27E-5 * \frac{318}{101350} \\ &= 7.122 \text{ E-8 meters} \end{aligned}$$

Approach 3:

One mol of air contains $6.022 \text{ E} +23$ molecules (Avogadro's Number). If air contains 78.08 % N_2 (Mol. Wt. 28), 20.95 % O_2 (Mol. Wt. 32) and 0.93 % Ar (Mol. Wt. 40), the average molecular weight of air is 28.94 g/mol. The density of air at 25 °C is 1.1744 kg/m^3 (Holman, 1990). One mol of air then occupies 0.02462 m^3 . This implies each molecule in air has average volume of 4.092 E-26 m^3 in which it can move before hitting another molecule. So taking cube root we can find mean free path ℓ as 3.446 E-9

meters. The density of air at 45 °C is 1.109816 kg/m³ (Holman, 1990). So one mol of air occupies 0.02607 m³. Each molecule has average volume of 4.33 E -26 m³. So the mean free path ℓ at 318 K is 3.5116 E-9 meters.

4.5.2 Verification of the Existing Model:

From the above calculations for mean free path, we can now find out the Knudsen number and can check the continuity of as model.

Approach 1:

Case 1: from equation (4.9)

$$\begin{aligned} \text{Kn} &= (153 \times 10^{-6}) / (6.6253 \times 10^{-8}) \\ &= 2309 \end{aligned}$$

Case 2: $\text{Kn} = (153 \times 10^{-6}) / (7.134 \times 10^{-8})$

$$= 2145$$

Approach 2: From equation (4.9)

Case1 $\text{Kn} = (153 \times 10^{-6}) / (6.675 \times 10^{-8})$

$$= 2290$$

Case 2 $\text{Kn} = (153 \times 10^{-6}) / (7.122 \times 10^{-8})$

$$= 2148$$

Approach 3:

$\text{Kn} = (153 \times 10^{-6}) / (3.5116 \times 10^{-9})$

$$= 43570$$

Table 4.2 Knudsen Numbers for Different Models.

| Model | Air Temperature Deg C | Knudsen Number | Allowable Microchannel Dimensions, Micro-meter |
|--------|--------------------------|-------------------|---|
| White | 25 | 2309 | 7.3 |
| | 45 | 2144 | 7.8 |
| Holman | 25 | 2290 | 7.35 |
| | 45 | 2148 | 7.85 |

From above calculations we can see that the dimensionless Knudsen Number is much greater than 110. Therefore we can still apply the viscous theory for our miniaturized channels. If we apply reverse technique to calculate the cut off characteristic dimension of micro-channels, we get $7.85 \mu\text{m}$ from first two approaches. That means we can apply viscous theory till this limit.

4.6 Convection Analysis Related to the Microchip

The cooling of chip is mainly accomplished by forced convection over the fins. For this processor chip a cooling fan is used.

4.6.1 Calculation of Air Velocity

The ambient air is drawn in by the fan and blown over the fins. When the air flows on the fins, it is equally divided into two ways. So the available flow rate is half the incoming because of symmetry. From Figure 4.1, we determine that the total available width for air to flow is 2.9 mm, and 0.93 mm is cumulative fin thickness for 10 fins.

The flow area available = 4.437 mm^2 .

Hence the velocity $U = \text{Vol. Flow} / A = 0.2358 \text{ m/s}$.

4.6.2 Reynolds Number

From Equation (2.11)

$$\text{Re}_L = \frac{U * L_1}{\nu} = 22.5$$

for a flow over a characteristic length of 1.45 mm, because of splitting of flow. Based upon this Reynolds number the flow is in a laminar regime. From White (1991) it is understood that boundary layer theory becomes fully complied when the length Reynolds number attains an order of 1000. Since microscale theory is not well developed yet, we use still laminar boundary layer equations, although Reynolds number is less than 1000.

4.6.3 Nusselts Number

For laminar flow over a flat surface, the following correlation is found to be applicable.

From Equation (2.10)

$$\text{Nu}_L = 0.664 * (\text{Re}_L)^{1/2} * (\text{Pr})^{1/3} = 2.815$$

For air Prandtl number $\text{Pr} = 0.712$

4.6.4 Heat Transfer Coefficient

The relation between Nusselt number & heat transfer coefficient h is given by

$$h = \text{Nu}_L * k_a / L_1$$

Substitution of various numbers yields

$$h = 25.40 \text{ W/m}^2 \text{ } ^\circ\text{C}$$

This is realistic for forced convection flows.

4.7 Heat Loss From Fins of Micro Heat Sink

The fin analysis is already explained in Section 2.7. The fin is exposed to the fluid, which is air at an ambient temperature of 45 Deg C. We illustrate here three cases of convection heat loss.

Case I

Use the maximum junction temperature of 80 Deg C., to get an upper bound of heat loss. Therefore from Equation (2.21), it is found that the temperature of tip is 79.7111 Deg C. The heat loss from both surfaces of each fin is 14.6 milli-Watts obtained using Equation (2.20) and from ten interior fins is 146 mW.

Case II

Here we use the calculated chip surface temperature, the contact resistance and the conduction through the sink base to obtain the temperature at base of fin to be 68.997 Deg C. It has been assumed that all air passes through the gap between the fins. To get lower bound we adopt the fin to be exposed to ambient air at 45 Deg C, the temperature at the tip is found from Equation (2.21) to be 68.994 Deg C. And the heat lost from each fin will be 10.2 mW from Equation (2.20) and from 10 fins as 102 mW.

4.8 Convection Results

Convection results for two cases as a parametric study is tabulated below.

Table 4.3 Comparison of convection heat losses for various cases.

| Case # | T _j | U m/s | Re | h | T _f | Q mW |
|--------|----------------|-------|------|------|----------------|------|
| 1 | 80 | 0.236 | 22.5 | 25.4 | 79.7 | 146 |
| 2 | 68.99 | 0.236 | 22.5 | 25.4 | 68.98 | 102 |

Figure 4.5 shows the variation of heat loss with varying air inflow. The airflow available is varied from 0.05 to 1.05 mm³/s.

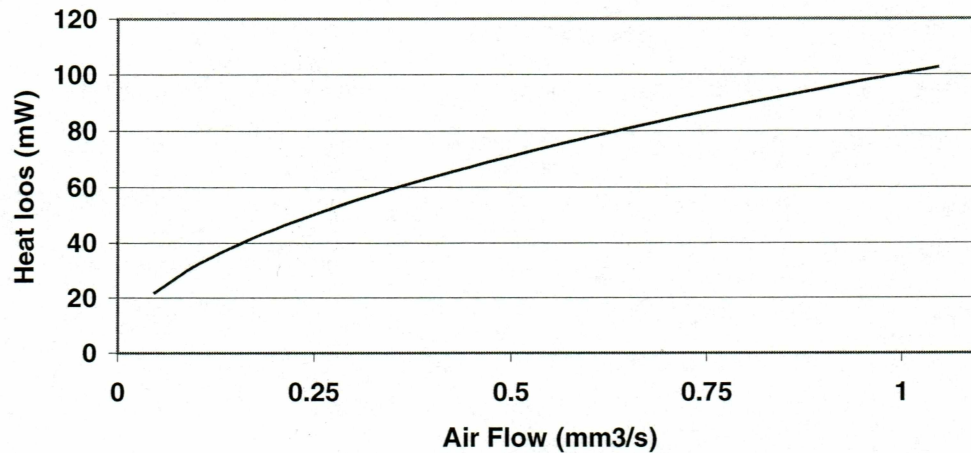


Figure 4.5 Variation of heat loss with varying airflow over the heat sink.

From this analysis we conclude that forced convection heat sink is perhaps an overkill (5mW necessary and its shows it can dissipate 150 mW) for the cooling of this microscale chip.

This leads us to believe that a natural convection and radiation heat sink would be better option for such small heat dissipation. Furthermore this will be economical design since we don't have to manufacture miniature motors and fans, which might add up the cost significantly high.

4.9 Radiation Analysis in Microchannels

For electronic devices operating at low temperatures, radiation plays a major role in heat dissipation from fins. Convection and radiation from heat sinks coexist, and when radiation is the primary cooling mode, the contribution due to natural convection cooling may become substantial. Also having high emissivity of heat sink surfaces, can significantly improve radiational heat transfer.

The heat loss due to radiation is given by Equation (2.22)

Considering the geometry of the fins on the heat sink, radiation will take place from the tip area, both side surface areas and from the base area. The tip will radiate heat to the surroundings with a full view factor ($F_A = 1$). But the base and side surfaces are restricted because of close spacing of fins. The side surfaces of fins will radiate a fraction given by a view factor as explained earlier in section 3.5.

View factor relation for identical, aligned rectangles directly opposite to each other is given by (Suryanarayana, 1995) Equation (2.23)

Where for our case; $x = L/d = 2.9/0.153 = 18.95$

$$y = w/d = 1.5/0.153 = 9.8$$

Here we have assumed one plane to be the side surface of one fin and the other plane is the opposite face of the other fin. The radiation is from fin side surface to air. Using Equation (2.23), the view factor for fin side surface yields $F_{1-3} = 0.86$. Emissivity of black paint heat sink aluminum is 0.9. Using the same theory view factor between the face and the bottom is calculated to be $F_{1-2} = 0.03$. Hence $F_{1-4} = 0.11$.

Let us consider two cases based upon two different surface temperatures.

Case I:

Tip Temperature of 352.711K, Base temperature of 352.99942K. The ambient air temperature is 318 K. There are 10 fins having tip area of 0.2967 mm^2 each, 18 faces of view factor 0.11 and 2 faces with view factor of 1 of area 4.35 mm^2 each, total base area available for radiation is 2.4273 mm^2 with view factor of 0.03 and 20 sides of fins having area of 0.1395 mm^2 each with view factor of 1. The heat lost from 10 fins tip area is 0.056 mW, from 20 faces heat loss will be 0.3 mW, from side area of fins 0.058 mW and from base area 0.0026 mW. So the cumulative radiation will be 0.8 mW considering emissivity to be 0.07 and the distribution of radiative heat transfer from various surfaces are shown in Figure 4.6.

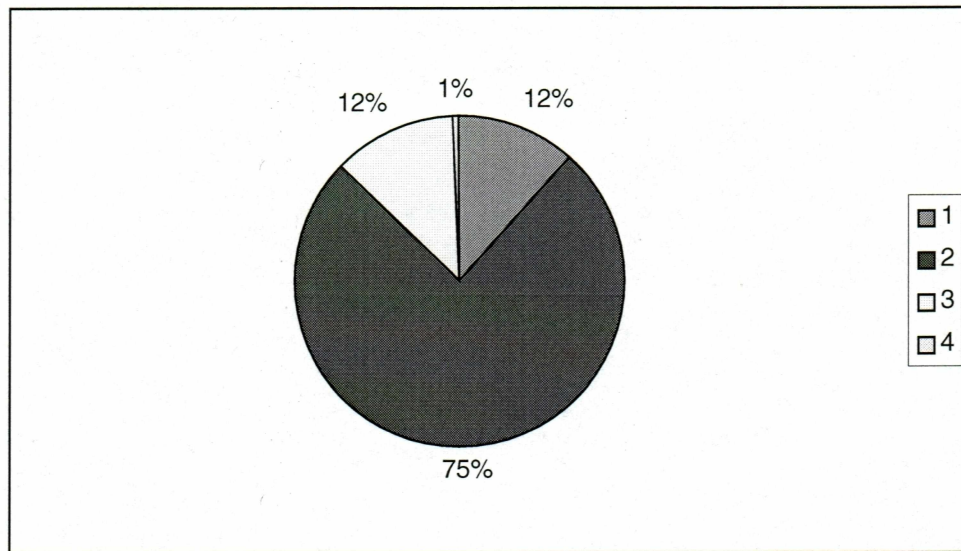


Figure 4.6 Distribution of radiation loss in Micro Heat sink.

Note: 1 : Radiation heat loss from Tip of Fins
2 : Radiation heat loss from Face of Fins
3 : Radiation heat Loss from Side of Fins
4: Radiation heat loss from Base Area.

4.9.1 Effect of Varying Emissivity

One can increase the radiative loss by improving the emissivity of surface by applying proper paints. This is normally done for heat sinks utilizing natural convection cooling. Therefore, the emissivity of extended surface was varied from 0.05 to 0.98 and the heat loss from radiation is depicted in Figure 4.7.

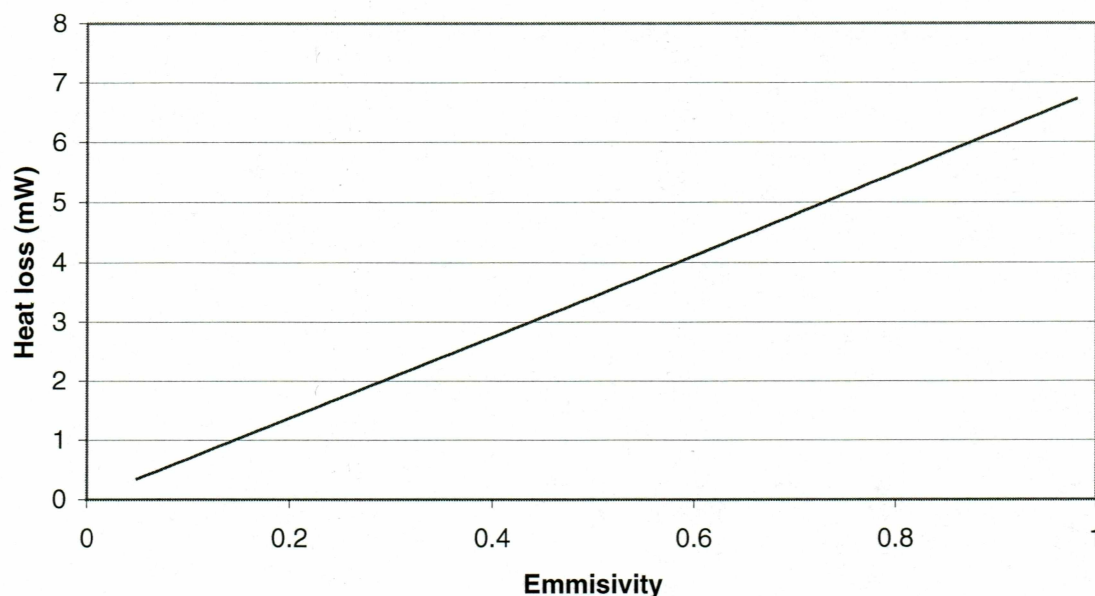


Figure 4.7 Effect on Heat Loss by Radiation with different emissivities.

From Figure 4.7 it is apparent that with an emissivity of about 0.73 we will be able to dissipate 5 mW, which is what our design calls for.

Case II:

Tip temperature of 340 K, Base temperature of 341 K. The geometry and ambient air temperature remains the same as in Case I. The total heat loss due to radiation in this case will be 0.285 mW. With high emissivity paint (0.98) the radiation loss can be increased to 4 mW.

4.10 Alternate Design of the Heat Sink for Microchip

Practically it is very hard to design a fan which is very small in dimensions as it shoots up the cost for heat sink in total. So we have to find out other economical ways like paintings with high emissivity materials. It is also important to see the role of natural

convection in place of forced one. Now just taking radiation and free convection into account we wish to explore the magnitude of heat dissipation that is possible. For free convection we assumed lower heat transfer coefficient of $5 \text{ w/m}^2\text{K}$ and for radiation we assumed that fins were painted with coatings having emissivity of 0.9. The ambient air temperature was 45°C . The graph below shows the comparison of free convection and radiation heat loss with varying fin surface temperature. This is a good comparison of natural convection versus radiation.

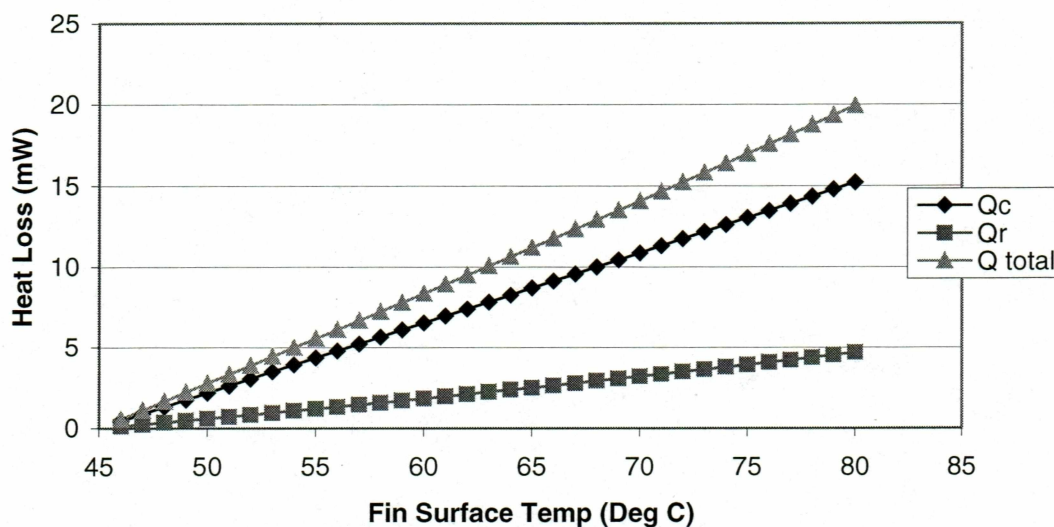


Figure 4.8 Effect of varying fin surface temperature on heat loss by free convection and radiation.

Note : Q_c is heat loss by natural Convection

Q_r is heat loss by radiation

From Figure 4.8, it can be easily seen that as the surface area available for heat transfer goes on decreasing, radiation plays dominant role. It can be also seen that to dissipate 5 mW of heat just 9°C temperature rise will be sufficient.

4.11 Numerical Analysis for Micro Scale Modeling

For 2D analysis, our first attempt was with a 1.5 mm x 3 mm computational domain. But upon running Fluent we were unable to find the detailed flow field in this tiny domain. Therefore we adopted a non-dimensionalization technique. In this technique we use a larger domain but change the length scale to match the Reynolds number. In this run we used grid having 10000 quadrilateral cells and 10201 node elements. After checking the mean free path length for gas molecules and if the continuum theory holds, we can employ this theory of non-dimensionlization.

4.11.1 Reynolds Number Matching

If we match the actual Reynolds number over a fin to our model Reynolds number while simulating in Fluent the fluid dynamic and heat transfer results will be unaffected. So if we simulate the boundary conditions such as inlet velocity of air to match the exact Reynolds number then we can succeed in making computations for the microscale domain. The actual Reynolds number is given by

$$\text{Re}_{\text{actual}} = \frac{U_{\text{actual}} L_1}{\nu} \quad (4.15)$$

Now we have to match this to simulated Reynolds number

$$\text{Re}_{\text{simulated}} = \frac{U_{\text{simulate}} L_2}{\nu} \quad (4.16)$$

Equating both the Reynolds number we get

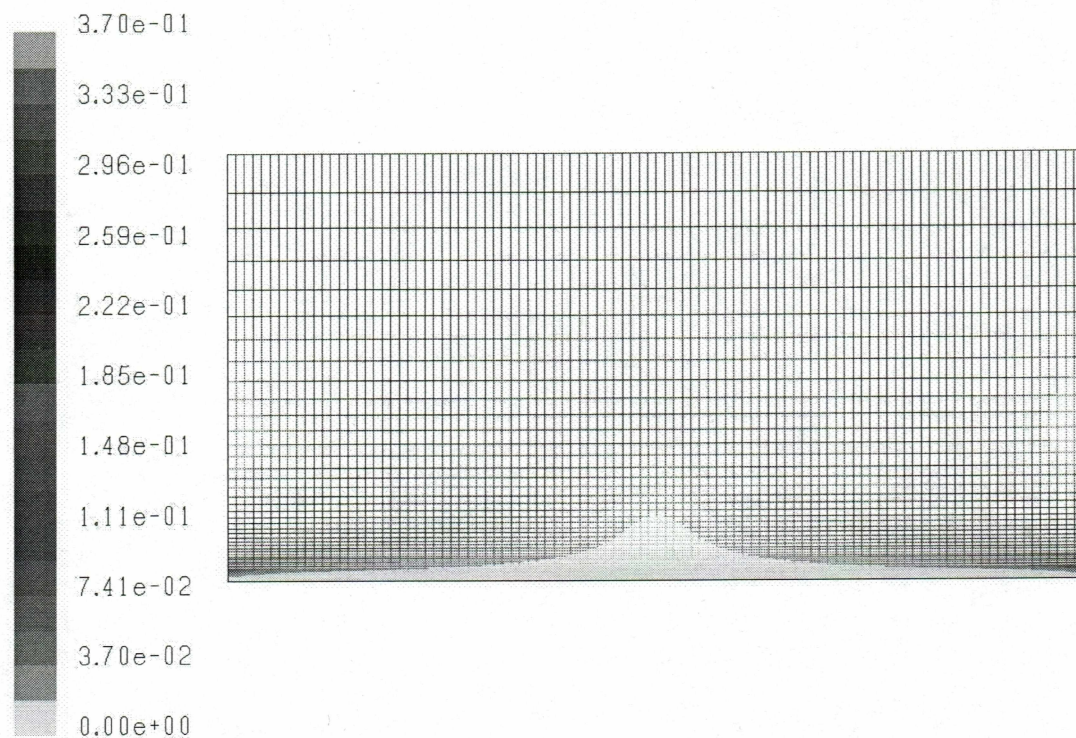
$$U_{\text{actual}} L_1 = U_{\text{simulated}} L_2 \quad (4.17)$$

In Fluent we created a domain of 0.5 m x 1 m. So $L_2 = 0.5$ m.

We know the actual velocity, which we have already found out by scaling to be 0.2358 m/s and length of 1.5 mm.

Thus the input velocity for Fluent is 0.691 mm/s from equation (4.17). After running the case we will get the velocity profile. To get the actual velocity from this velocity profile

we have to multiply by a scaling factor of $(L_2/L_1) = (0.5/1.5 \times 10^{-3}) = 333.33$. For Nusselt number plot there will not be any change as this is a function of Reynolds number and Prandtl number only and both of them match. And to get heat transfer coefficient we have to multiply by the scaling factor of 333.33



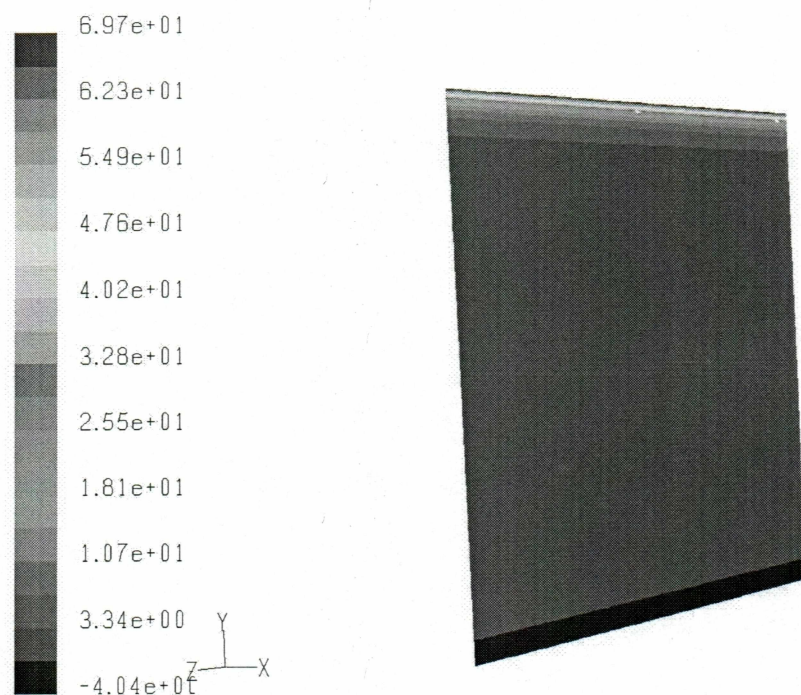
Contours of Velocity Magnitude (m/s)

May 05, 2003
FLUENT 6.0 (2d, dp, segregated, lam)

Figure 4.9 Counters of velocity for microscale fins.

From Figure 4.9 we can see that the velocity profile is getting split up into two symmetrical equal flows. When the air reaches to the wall, velocity gets reduced a lot and at the wall it is stationary. At the outlet the velocity is increased a lot to keep volume flow rate constant. The range of velocity is 0-0.7 m/s.

For 3D analysis, we used the same domain as used for macroscale in chapter 3. In our domain the characteristic length is 25 mm, and in actual case it is 1.5 mm. Therefore, after matching Reynolds number, we found the velocity for simulation is to be 1.4 cm/s. The results of this run are summarized below.



Contours of Surface Heat Transfer Coef. (w/m²-k)

Jul 16, 2003
FLUENT 6.0 (3d, dp, segregated, lam)

Figure 4.10 Contours of surface heat transfer over the fin for velocity of 1.4 cm/s.

From Figure 4.10, we can conclude that the heat transfer gradually decreases from the leading edge. The range of h is from 69.7 to 0 W/m²K. to get the actual h value for microscale we have to multiply by the scaling factor of $(L_2/L_1) = 25/1.5 = 16.67$. The heat loss by the fin is given 0.059 watts and from the bottom it is 0.003 watts. After multiplying by scaling factor we get the total heat loss by all 10 fins is 268 mW.

CHAPTER FIVE

CONCLUSIONS

The following conclusions are made after reviewing the results upon completion of this investigation.

A) From Macro Scale Modeling:

1. The total heat generated in Pentium III chip is 23 W. By analytical results we are getting heat dissipation of 11.9 to 43.3 W from forced convection. By numerical approach we are getting heat dissipation in the range of 38.8 to 46.6 W.
2. Transient temperature curve predicts a uniform temperature of 69 to 68.2 °C, when steady state is reached. Steady state is attained in the whole sink in 47 minutes.
3. Radiation heat loss is also increased from 0.5% (0.137 W) to 8.3% (1.91 W) by applying different coatings / paints of high emissivity.
4. Heat transfer coefficient h for analytical results varies from 18 to 22.7 W/m²C. For numerical approach it varies from 32 to 34 W/m²C from two-dimensional analysis, and 219 (leading edge) to 19 W/m²C from three-dimensional analysis.
5. In case of natural convection and radiation for Pentium II processor, the sink is able to dissipate heat of 12 W when the case temperature is 69 °C.

B) From Micro Scale Modelling:

6. The heat sink designed for miniaturized processor chips by scaling laws will dissipate 102 mW of heat by analytical approach and 268 mW by numerical approach, which is much more than 5 mW of heat, which is to be dissipated.
7. Knudsen number is nearly 2200 for microscale heat sink.
8. Continuum theory holds good until gap dimension between the fins approaches of 7.8 micrometer.
9. In micro heat sink, the steady state is reached 18 milliseconds for whole heat sink.
10. Micro heat sink can dissipate 5 mW by radiation and natural convection with a 9°C temperature rise.
11. Correlations for natural convection are over predicting ($\sim 20 \text{ W/m}^2\text{C}$) the heat transfer coefficient values for low Rayleigh number. Therefore, future study is required for finding out the correlations for micro dimensions.

REFERENCES

Bar-Cohen, A., Kraus, A. D., (1990), "Advances in Thermal Modeling of Electronics Components and Systems", Volume 2, ASME Press, New York.

Bar-Cohen, A., Kraus, A. D., (1990), Advances in Thermal Modeling of Electronic Components and Systems, Vol. II, ASME Press.

Bejan, A., (1993), Heat Transfer, John Willey & Sons Inc., New York.

Beskok, A., Karniadakis, George Em, (1999), "A Model for Flows in Channels, Pipes, and Ducts at Micro and Nano Scales", Microscale Thermophysical Engineering, Taylor and Francis.

Carlen, Edwin T., Mastrangelo, C.H., October (2002), "Surface Micromachined Paraffin-Actuated Microvalve", Journal of Microelectromechanical Systems, Vol.11, No.3, ASME/IEEE.

Fabis, P.M., Windischmann, H., (2000), "Thermal Management Enhancement for GaAs Devices Using CVD Diamond Heat Spreader in a Plastic Package Environment", Journal of Electronic Packaging, Vol.122, pp. 92-96.

Holman, J. P., (1990), "Heat Transfer", McGraw Hill, New York.

<http://www.electro-optical.com>, Material Emissivity Properties.

Incropera F.P., Dewitt D.P., (2002), "Fundamentals of Heat and Mass Transfer", John Wiley & Sons, New York.

Intel (2001), Data sheet, Revision 8, Section 4.0, "Thermal Specifications and Design Considerations", Pentium III processor for the PGA 370 Socket at 500 MHz to 1.1 GHz, pp. 56-82.

Intel (2003), Data sheet, "Thermal Specifications", Pentium II processor – Low Power, pp. 48-50.

Jamina, A., (2003), Practical Guide to the Packaging of Electronics, Marcel Dekker Inc., New York.

Ju, Y.S., Goodson, K.E., (1999), "Microscale Heat Conduction in Integrated Circuits and Their Constituent Films", Kluwer Academic Publishers, Boston.

Kraus, A., D., Bar-Cohen, A., (1983), "Thermal Analysis and Control of Electronic Equipment", McGraw Hill Company, New York.

Kraus, A. D., Bar-Cohen A., (1995), Design and Analysis of Heat Sinks, John Wiley & Sons, Inc., New York.

Martin, M.J., Kurabayashi, K., Boyd I., D., (2001), "Measurement of Lift and Drag on MEMS scale Airfoils in Slip Flow", Proceedings of ASME Fluids Engineering Division Summer Meeting, New Orleans, Louisiana.

Sabry, M., N., (2000), "Scale Effects on Fluid Flow and Heat Transfer in Microchannels", IEEE Transactions on Components and Packaging Technologies, Vol.23, No.3.

Seri Lee, (1995), "How to select a Heat Sink", Electronics Cooling, Vol.1, No.1, pp.10-14.

Seri Lee, (1998), "Calculating Spreading Resistance in Heat Sinks", Electronics Cooling, Article published in January.

Suryanarayana, N., V., (1995), "Engineering Heat Transfer", West Publishing Company, MN.

Tummala, R., R., (2001), "Fundamentals of Microsystems Packaging", McGraw Hill, Boston.

White F.M., (1991), "Viscous Fluid Flow", McGraw Hill, New York.